Stereoselectivity and Structural Characterization of an Imine Reductase (IRED) from *Amycolatopsis orientalis*

Godwin A. Aleku,[a†] Henry Man,[b†] Scott P. France[a], Friedemann Leipold,[a] Shahed Hussain,[a] Laura Toca-Gonzalez[a], Rebecca Marchington[a], Sam Hart,[b] Johan P. Turkenburg,[b] Gideon Grogan[b] and Nicholas J. Turner[a]**

[a]School of Chemistry, University of Manchester, Manchester Institute of Biotechnology, 131 Princess Street, Manchester, M1 7DN, UK.

[b]York Structural Biology Laboratory, Department of Chemistry, University of York, YO10 5DD York, UK.

Corresponding Authors:

*(G.G.) Email: gideon.grogan@york.ac.uk

*(N.J.T.) Email: nicholas.turner@manchester.ac.uk

Supporting Information

Section S1. General

Solvents used were of HPLC grade and when necessary solvents were further dried over molecular sieves. Column chromatography was performed on silica gel (Fluka (Buchs, Switzerland), 220-440 mesh). Spectra from ^{1}H and ^{13}C NMR runs were recorded on a Bruker Avance 400 instrument (400 MHz for ^{1}H and 100 MHz for ^{13}C) in $CDCl_3$ or CD_3OD using residual protic solvent as an internal standard. Reported chemical shifts (δ) (in parts per million (ppm) are relative to the residual protic solvent signal ($CHCl_3$ in $CDCl_3$, ^{1}H = 7.26; $CDCl_3$, ^{13}C = 77.0; CHD_2OD in CD_3OD, ^{1}H = 3.31; CD_3OD, ^{13}C = 49.0).

High-resolution mass spectrometry (HRMS) was recorded using a Waters LCT time-of-flight mass spectrometer, connected to a Waters Alliance LC (Waters, Milford, MA, USA). Data were processed with Waters Masslynx software. Samples for IR spectroscopy were run on a Nicolet 5700 FT-IR (Thermo Electron, Madison, WI, USA) using a Smart Orbit Diamond accessory.

Determination of optical rotation was performed on an AA-100 polarimeter at 25°C with the solvent and concentration stated. Chiral normal phase HPLC was performed on an Agilent system (Santa Clara, CA, USA) equipped with a G1379A degasser, G1312A binary pump, a G1367A well plate autosampler unit, a G1316A temperature controlled column compartment and a G1315C diode array detector. CHIRALPAK®IA, CHIRALPAK®IC and CHIRALPAK®IE Analytical (all Daicel (Osaka, Japan), 250 mm length, 4.6 mm diameter, 5 μm particle size) as well as CHIRALCEL®OD-H Analytical (Daicel (Osaka, Japan), 250 mm length, 4.6 mm diameter, 5 μm particle size) columns were used. The typical injection volume was 10 μl and chromatograms were monitored at 265 nm. All solvent mixtures are given in (v/v) ratios.

GC analysis was performed on a Agilent 6850 GC (Agilent, Santa Clara, CA, USA) with a flame ionization detector (FID) and autosampler equipped with a 25 m CP-Chirasil-DEX CB column with 0.25 mm inner diameter and 0.25 μm film thickness (Agilent, Santa Clara, CA, USA). Where necessary, samples were derivatized using acetic anhydride with an excess of triethylamine at room temperature prior to analysis on the GC-FID.

Section S2. Cultivation and Purification of *Ao*IRED.

S2. 1. Strains and plasmids

Escherichia coli DH5α [F^- ϕ80*lac*ZΔM15 Δ(Δ*lac*ZYA-argF) U169 *rec*A1 *end*A1 *hsd*R17(r_k^-, m_k^+) *pho*A *sup*E44 *thi*-1 *gyr*A96 *rel*A1 λ^-] was used from our own strain collection. *E. coli* XL1-Blue [*rec*A1 *end*A1 *gyr*A96 *thi*-1 *hsd*R17(r_k^-, m_k^+) *sup*E44 *rel*A1 *lac* [F′ *proAB* *lacI*^{q}Z*ΔM15* Tn*10* (Tet^r)]] and *E. coli* ArcticExpress (DE3) [F^- *ompT hsd*S(r_B-m_B-) *dcm*$^+$ Tet^r *gal* λ(DE3) *end*A Hte [*cpn10 cpn60* $Gent^r$] were sourced from Agilent (Santa Clara, CA, USA). *E. coli* BL21 (DE3) [F^- *ompT hsd*S_B(r_B-m_B-) *gal dcm rne*131 (DE3)] was purchased from Merck (Darmstadt, Germany). Chemically competent *E. coli* cells were purchased from New England Biolabs (Ipswich, MA, USA). pET-28a(+) was purchased from Novagen (Darmstadt, Germany). The Chaperone Plasmid Set containing the plasmids pG-KJE8, pGro7, pKJE7, pG-Tf2, and pTF16 was purchased from TaKaRa Bio Inc. (Otsu, Japan). pET-28a(+) was purchased from Novagen (Darmstadt, Germany). PUC-His-*Ao*IRED was synthesised by Biomatik (Cambridge, Ontario, Canada).

S2. 2. Cloning and expression of *Ao*IRED and mutants

Optimization of the IRED gene sequence

To achieve high protein expression level, *Ao*IRED gene sequence was codon-optimised for expression in *E. coli*. The optimized (opt) sequence shares 78.47% identity to the original (wt) sequence. An alignment of original and optimised sequences is shown below, optimized codons highlighted in red.

```
opt ATGACCGACCAGAACCTGCCGGTTACCGTGGCGGGTCTGGGCCCGATGGGCTCCGCTCTG 60
wt  ATGACCGATCAGAACCTCCCGGTGACCGTCGCCGGGCTCGGCCCGATGGGCTCCGCGCTC 60
    ******** ******** ***** ***** ** ** ** ***************** **

opt GCGGCTGCACTGCTGGACCGTGGTCACGACGTTACTGTTTGGAACCGCTCTCCGGGCAAA 120
wt  GCCGCCGCCCTGCTCGACCGCGGTCACGACGTGACCGTGTGGAACCGCTCCCCCGGCAAG 120
    ** ** ** ***** ***** ********** ** ** ********** ** *****

opt GCAGCACCGCTGGTGGCTAAAGGTGCGCGTCAGGCGGACGACATCGTTGACGCGGTTAGC 180
wt  GCCGCCCCCTTGGTGGCGAAAGGCGCGCGGCAGGCGGACGACATCGTGGACGCGGTGTCC 180
    ** ** **  ******* ***** ***** ***************** ********   *

opt GCGTCCCGCCTGCTGGTTGTGTGCCTGGCGGACTACGATGCGCTGTATAGCGCACTGGGT 240
wt  GCGAGCCGTCTGCTCGTGGTCTGCCTCGCCGACTACGACGCGCTTTACTCCGCGCTCGGC 240
    ***  *** ***** ** ** ***** ** ******** ***** **   *** ** **

opt CCGGCTCGTGAAGCGCTGCGTGGTCGTGTTGTTGTTAACCTGAACTCTGGCACCCCGAAA 300
wt  CCCGCGCGGGAAGCCTTGCGCGGCCGCGTAGTGGTGAACCTGAATTCCGGCACGCCGAAG 300
    ** ** ** *****  **** ** ** ** ** ** ******** ** ***** *****

opt GAAGCGAACGAAGCTCTGCGTTGGGCGGAGCGTCACGGTACTGGTTACCTGGACGGTGCG 360
wt  GAGGCGAACGAAGCTCTCCGATGGGCCGAGCGACACGGAACGGGCTATCTCGACGGCGCC 360
    ** ************** ** ***** ***** ***** ** ** ** ** ***** **

opt ATCATGGTTCCGCCGGCAATGGTTGGTCACCCAGGCTCTGTTTTCCTGTACTCTGGCTCT 420
wt  ATCATGGTTCCCCCCGCGATGGTCGGCCACCCCGGCTCGGTCTTCCTCTACAGCGGTTCC 420
    *********** ** ** ***** ** ***** ***** ** ***** ***   ** **

opt GCTGAAGTTTTCGAAGAATACAAAGAAACCCTGGCTGGCCTGGGCGACCCGGTTCACCTG 480
wt  GCCGAGGTTTTCGAGGAATACAAGGAGACATTGGCCGGTCTGGGTGATCCGGTCCATCTC 480
    ** ** ******** ******** ** **  **** ** ***** ** ***** ** **

opt GGTACTGAAGCGGGCCTGGCAGTTCTGTACAACACCGCGCTGCTGTCTATGATGTACAGC 540
wt  GGCACGGAAGCCGGCCTCGCCGTGCTGTACAACACCGCGTTGCTGAGCATGATGTACTCG 540
    ** ** ***** ***** ** ** *************** *****   *********

opt TCTATGAACGGTTTTCTGCATGCTGCGGCACTGGTGGGTTCTGCAGGTGTTCCGGCTGCG 600
wt  TCGATGAACGGTTTCCTCCACGCCGCCGCGCTGGTCGGCAGTGCCGGGGTCCCGGCGGCC 600
    ** *********** ** ** ** ** ** ***** **   *** ** ** ***** **

opt GAGTTCACCAAACTGGCTGTTGACTGGTTTCTGCCGGCTGTGATCGGTCAGATCATCAAA 660
wt  GAATTCACGAAGCTCGCCGTCGACTGGTTCCTGCCCGCGGTGATCGGACAGATCATCAAG 660
    ** ***** ** ** ** ** ******** ***** ** ******** **********
```

```
opt GCGGAAGCGCCGACCATCGACGAAGGCGTTTATCCGGGCGATGCGGGTTCTCTGGAAATG 720
wt  GCGGAGGCGCCCACCATCGACGAAGGCGTGTACCCCGGTGACGCCGGTTCGCTGGAAATG 720
    ***** ***** ***************** ** ** ** ** ** ***** *********

opt AACGTGACTACTCTGAAACACATCATCGGCACCTCTCAGGAACAGGGTGTTGATACCGAA 780
wt  AACGTCACGACACTGAAGCACATCATCGGAACCAGCCAGGAGCAGGGCGTCGACACCGAG 780
    ***** ** ** ***** ********** ***   ***** ***** ** ** *****

opt ATCCCGGTGCGTAACAAAGAGCTGCTGGATCGTGCAGTTGCAGCGGGTTTCGGCGAATCT 840
wt  ATCCCGGTCCGCAACAAGGAACTTCTGGACCGGGCCGTCGCCGCCGGGTTCGGCGAGAGC 840
    ******** ** ***** ** ** ***** ** ** ** ** ** ** ********

opt TCTTACTATTCTGTTATCGAACTGTGGCGTTAA 873
wt  AGCTATTACTCGGTGATCGAACTGTGGAGGTGA 873
       ** ** ** ** ********** * * *
```

Cloning of the *Ao*IRED gene and creation of mutants

The codon-optimized gene sequence encoding *Ao*IRED was synthesized by Biomatik (Cambridge, Ontario, Canada) and sub-cloned into pET28a (+) vector using *Nde*I and *Xho*I restriction sites to form pET 28a-His-*Ao*IRED plasmid.

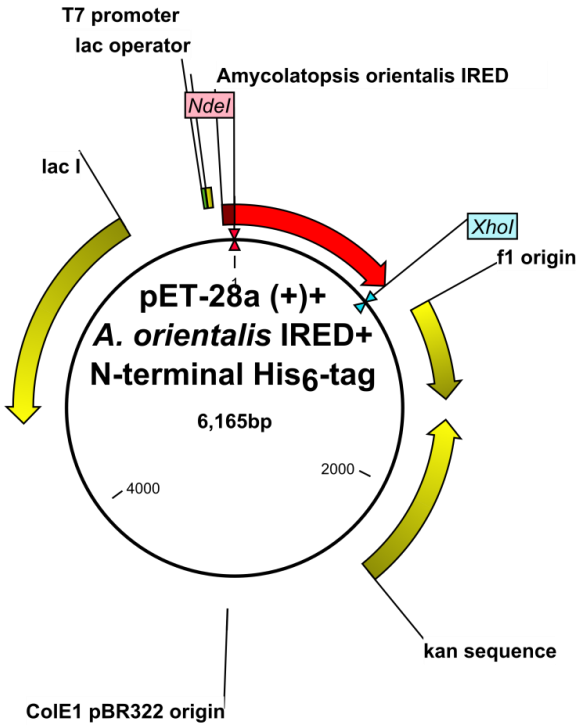

Figure S1. Plasmid map of pET-His-*Ao*IRED

Native *Ao*IRED plasmid served as the template for the creation of mutants using the Stratagene Quickchange site directed mutagenesis protocol. Successful cloning and creation of the target mutations were confirmed by sequencing.

List of primers for construction of AoIRED mutants

***Ao*IRED N171A**
Sense: 5'-GTTCTGTACGCGACCGCGCTGCTGTCTATG-3'
Antisense: 5'-CAGCGCGGTCGCGTACAGAACTGCCAGGCC-3'

***Ao*IRED N171D**
Sense: 5'-GTTCTGTACGATACCGCGCTGCTGTCTATG-3'
Antisense: 5'-CAGCGCGGTATCGTACAGAACTGCCAGGCC-3'

***Ao*IREDY179A**
Sense: 5'-TCT ATG ATG GCG AGC TCT ATG AAC GGT TTTC-3'
Antisense: 5'-TCA TAG AGC TCG CCA TCA TAG ACA GCA GCGC-3'

***Ao*IRED Y179F**
Sense: 5'-TCTATGATGTTTAGCTCTATGAACGGTTTTC-3'
Antisense: 5'-TCATAGAGCTAAACATCATAGACAGCAGCGC-3’

***Ao*IREDN241A**
Sense: 5'-CTGGAAATGGCGGTGACTACTCTGAAAC-3'
Antisense: 5'-AGTAGTCACCGCCATTTCCAGAGAACCC-3'

S2. 3. Purification of *Ao*IRED

The general procedure for the purification of *Ao*IRED is detailed in the Experimental Section of the Manuscript.

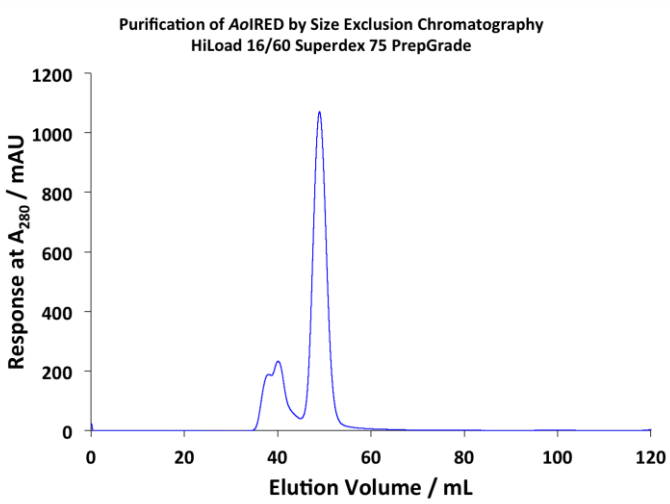

Figure S2. Chromatagram of *Ao*IRED purified by SEC using a HiLoad 16/60 Superdex 75 PrepGrade. The main peak with an elution volume of 50 mL suggests a species with a molecular weight of approximately 60 kDa.

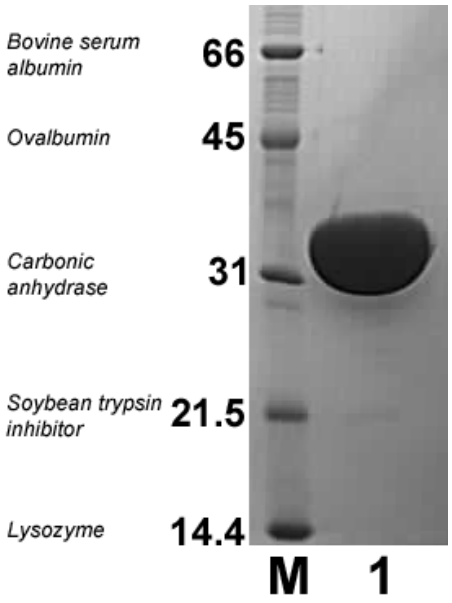

Figure S3. SDS-PAGE analysis of the purified *Ao*IRED by SEC. Lane M is the low weight molecular marker from BioRad and Lane 1 is the purified *Ao*IRED. Coomassie Blue staining protocol was employed, followed by de-staining using a 6:3:1 mixture of water/methanol/acetic acid.

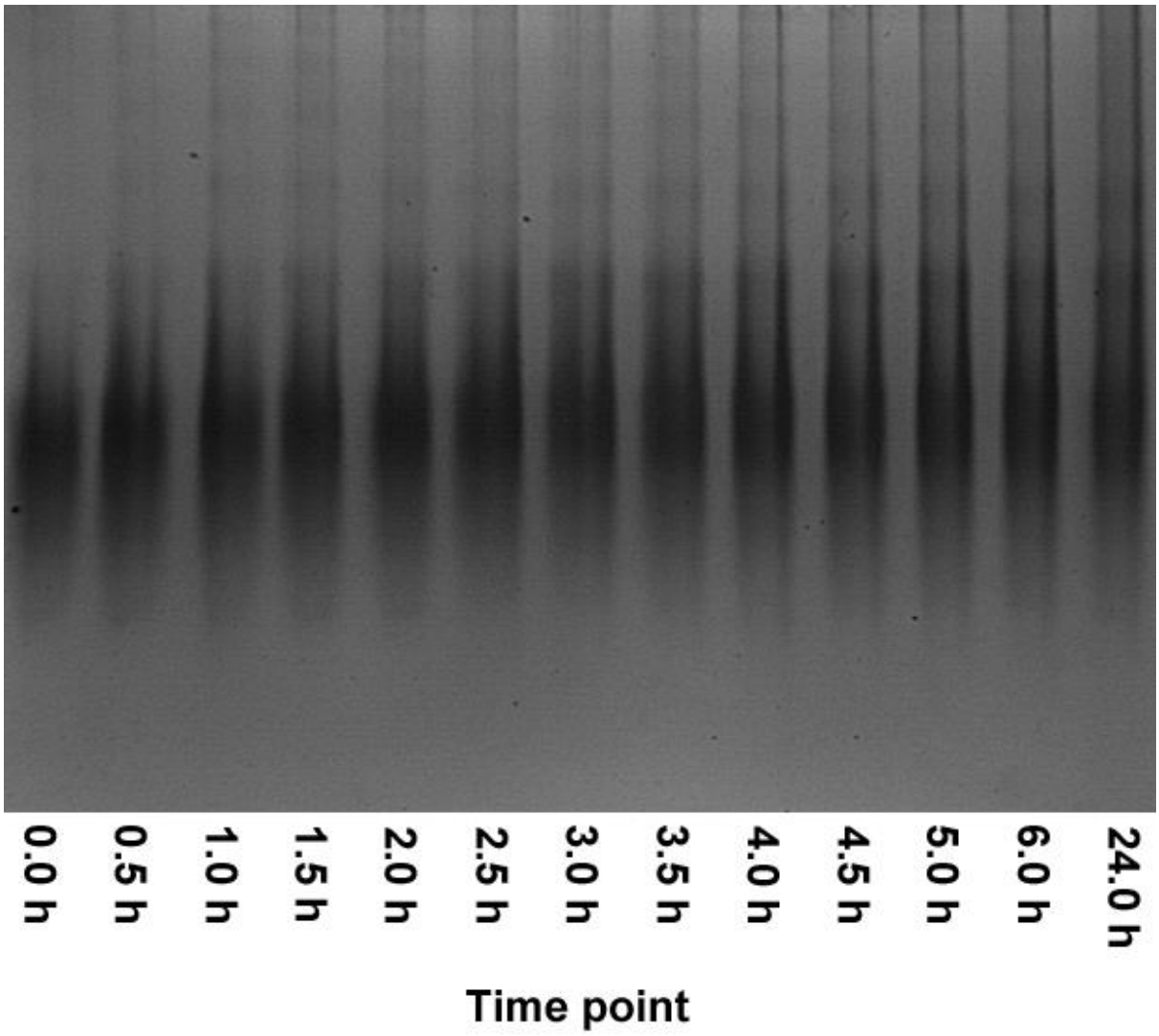

Figure S4. Native gel analysis analysis of the purified *Ao*IRED on storage. A gradual increase in smearing from left to right may be indicative of a conformational change in the protein, associated with the observed switch in stereoselectivity towards substrate **9**.

Section S3. Effect of pH and temperature on imine reducing activity of *Ao*IRED

The effect of pH and temperature on imine reducing activity and stability of *Ao*IRED was studied. For the determination of pH optimum, the activity of purified *Ao*IRED was measured and found to be optimally active at pH 7.5 (Figure S4). The pH stability of the enzyme was assessed after 2 h incubation in reaction buffers at 4°C; *Ao*IRED remained stable and active at pH values between 6 and 9. At enzyme concentrations below 2mg/ml and a pH of 7.5, 90% of *Ao*IRED's activity was retained after 4 weeks incubation at 4°C. The temperature optimum was determined analogously by measuring activity at temperatures ranging from 20 and 65°C at a constant pH of 7.5 for 5 mins, while thermostability of *Ao*IRED was assessed by measuring the residual enzyme activity following 2 h incubation at different temperatures. While temperature optimum was found to be 50 °C (Figure S4) and the enzyme was active over a wide temperature range (20-60°C) during a 5 mins assay, *Ao*IRED precipitated after 1h incubation at ≥40°C. We recommend that reactions employing *Ao*IRED may be carried out at temperature range between 25 and 37°C. We also observed that *Ao*IRED precipitates in buffers at protein concentration in excess of 10mg/mL after 8 h or longer incubation at 4°C.

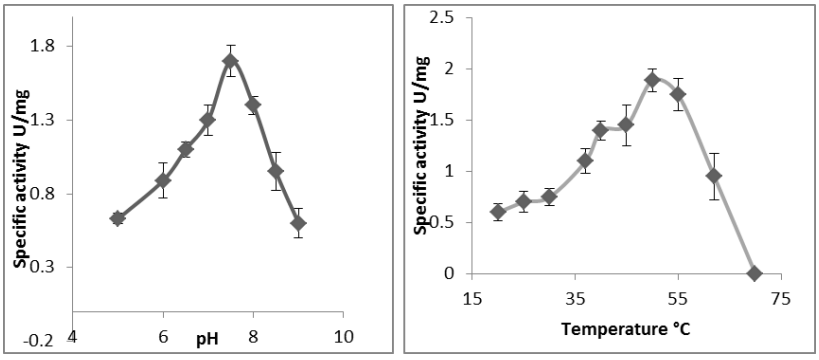

Figure S5. Effect of temperature and pH on the imine reducing activity of *Ao*IRED. The pH and temperature optimum were found to be 7.5 and 50°C respectively. Activities were measured in triplicate and error bars represent standard deviations. For determination of pH optimum, buffers used include 0.1M sodium citrate buffer (pH 5-6), 0.1M sodium phosphate buffer (pH 6.5 to 8), 0.1M Tris HCl buffer pH 8-9**.**

S4. Synthesis of imines and racemic amines

S4.1. Preparation of imines 3e and 3f.

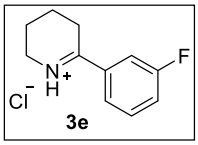

2-(*m*-fluorophenyl)-1-piperideinium chloride (3e)

A solution of *N*-Boc-2-piperidone (0.55 g, 2.76 mmol) in THF (10 mL) was cooled to -78°C under N_2 before (3-fluorophenyl)magnesium bromide (3.87 mL, 19.4 mmol) was added dropwise. The solution was stirred overnight. The reaction mixture was then warmed to room temperature before the addition of 1M HCl (10 mL). The phases were separated and the aqueous layer was extracted with CH_2Cl_2 (3 x 20 mL). The organic phases were then combined, dried over $MgSO_4$ and concentrated *in vacuo* to yield *tert*-butyl(5-oxo-5-(*m*-fluorophenyl)pentyl)carbamate (0.45 g, 1.54 mmol, 56%), which was then dissolved and stirred in trifluoroacetic acid (3 mL) for 4 hours. The reaction mixture was then cooled to 0°C before the pH was adjusted to pH 14 by addition of 10 M NaOH. The phases were separated and the aqueous layer was extracted with CH_2Cl_2 (3 x 15 mL). The organic layers were combined, dried over $MgSO_4$ and concentrated *in vacuo* to give the free base imine, which was dissolved in diethyl ether before addition of 2 M HCl/diethyl ether solution. The salt was then isolated by filtration and dried to give imine **3e** (0.32 g, 1.52 mmol, 55%) as its hydrochloride salt.

^{1}H NMR δ_H (400 MHz, CD_3OD) 7.80 – 7.73 (m, 2H), 7.82 – 7.76 (m, 1H), 7.71 (td, *J* = 8.0, 5.5 Hz, 1H), 3.93 – 3.87 (m, 2H), 3.37 – 3.29 (m, 2H), 2.10 – 2.02 (m, 4H); **^{13}C NMR** δ_C (100 MHz, CD_3OD) 184.2, 164.2 (d, *J* = 248.0 Hz), 135.2 (d, *J* = 8.0 Hz), 132.9 (d, *J* = 8.0 Hz), 125.2 (d, *J* = 3.5 Hz), 122.8 (d, *J* = 21.5 Hz), 116.1 (d, *J* = 24.5 Hz), 46.7, 29.4, 20.2, 18.1; **IR** υ_{max}/cm^{-1} 3052 (C-H), 2965(C-H), 2182 (C=N); **MS** *m/z* 178.4 $[M+H]^+$.

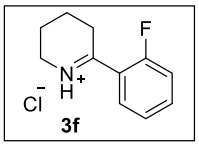

2-(*o*-fluorophenyl)-1-piperideinium chloride (3f)

1-Bromo-2-fluorobenzene (1.32 mL, 4.32 mmol) in THF (8 mL) was added dropwise to a mixture of magnesium (207 mg, 8.64 mmol) in THF (16 mL) and a drop of dibromoethane under N_2. This was stirred for 1.5 hours at 25°C to give (2-fluorophenyl) magnesium bromide, which was then added to a solution of *N*-Boc-2-piperidone (0.53 g, 2.68 mmol) in THF (10 mL) at-78°C. The mixture was stirred at -78°C overnight. The reaction mixture was then warmed to room temperature and 1M HCL (10 mL) was added. The organic layer was separated and the aqueous layer extracted with CH_2Cl_2 (3 x 20 mL). The organic layers were combined, dried over $MgSO_4$ and concentrated *in vacuo* to give *tert*-butyl(5-oxo-5-(*o*-fluorophenyl)pentyl)carbamate (0.52 g, 1.76 mmol, 66%) as a white solid, which was then dissolved and stirred in trifluoroacetic acid (3 mL) for 4 hours. The reaction mixture was then cooled to 0°C before the pH was adjusted to pH 14 by addition of 5 M NaOH. The phases were then separated and the aqueous layer was extracted with CH_2Cl_2 (3 x 15 mL). The organic layers were combined, dried over $MgSO_4$ and concentrated *in vacuo* to give the free base imine, which was dissolved in diethyl ether before addition of 2 M HCl/diethyl ether solution. The salt was then isolated by filtration and dried to give imine **3f** (0.35 g, 1.64 mmol, 61%) as a white powder.

^{1}H NMR δ_H (400 MHz, CD_3OD) 7.53 (td, J = 7.5, 1.5 Hz, 1H), 7.82 – 7.76 (m, 1H), 7.47 (td, *J* = 7.5, 1.0 Hz, 1H), 7.42 (ddd, *J* = 11.5, 8.5, 1.0 Hz, 1H), 3.93 – 3.88 (m, 2H), 3.30 – 3.25 (m, 2H), 2.11 – 1.99 (m, 4H); **^{13}C NMR** δ_C (100 MHz, CD_3OD) 182.8, 161.0 (d, *J* = 254.5 Hz), 137.7 (d, *J* = 9.5 Hz), 131.23, 126.7 (d, *J* = 3.5 Hz), 121.8 (d, *J* = 11.0 Hz), 118.2 (d, *J* = 22.0 Hz), 46.8, 22.1, 18.1, 18.0; **IR** υ_{max}/cm^{-1} 3053 (C-H), 2965 (C-H), 2158 (C=N); **MS** *m/z* 178.3 $[M+H]^+$.

S4. 2. Preparation of amines 4e and 4f.

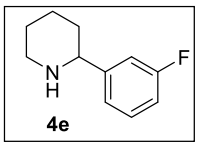

4e

2-(*m*-fluorophenyl)piperidine (4e): 3e (30 mg, 0.14 mmol) was dissolved in MeOH (1 mL). The mixture was cooled to 0°C before the flask was charged with $NaBH_4$ (11 mg, 0.28 mmol) and stirred for 30 minutes. Water (1 mL) was then added and the mixture was extracted with CH_2Cl_2 (3 x 5 mL). The organic phases were combined, dried over $MgSO_4$ and concentrated *in vacuo* to give **4e** (21 mg, 84% yield) as an oil.

^{1}H NMR δ_H (400 MHz, $CDCl_3$) 7.26 (td, *J* = 8.0, 6.0 Hz, 1H), 7.14 – 7.07 (m, 2H), 6.92 (tdd, *J* = 8.5, 2.5, 1.0 Hz, 1H), 3.59 (dd, *J* = 10.0, 2.5 Hz, 1H), 3.22 – 3.16 (m, 1H), 2.79 (td, *J* = 11.5, 3.0 Hz, 1H), 1.92 – 1.83 (m, 1H), 1.81 – 1.75 (m, 1H), 1.72 (bs, 1H), 1.69 – 1.61 (m, 1H), 1.58 – 1.39 (m, 3H); **^{13}C NMR** δ_C (100 MHz, $CDCl_3$) 163.1 (d, *J* = 245.5 Hz), 148.5 (d, *J* = 7.0 Hz), 129.9 (d, *J* = 8.5 Hz), 122.3 (d, *J* = 2.5 Hz), 113.9 (d, *J* = 21.0 Hz), 113.6 (d, *J* = 21.5 Hz), 61.9 (d, *J* = 1.5 Hz), 47.8, 35.2, 26.0, 25.5; **IR** υ_{max}/cm^{-1} 3339 (N-H), 2983 (C-H), 2852 (C-H); **HRMS** calcd. for $C_{11}H_{15}N$ 180.1189 [$M+H^+$], found 180.1279.

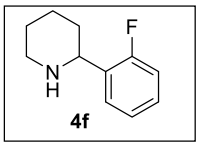

4f

2-(*o*-fluorophenyl)piperidine (4f): **3f** (30 mg, 0.14 mmol) was dissolved in MeOH (1 mL). The mixture was cooled to 0°C before the flask was charged with $NaBH_4$ (11 mg, 0.28 mmol) and stirred for 30 minutes. Water (1 mL) was then added and the mixture was extracted with CH_2Cl_2 (3 x 5 mL). The organic phases were combined, dried over $MgSO_4$ and concentrated *in vacuo* to give **4f** (23 mg, 0.13 mmol, 90%) as an oil.

^{1}H NMR δ_H (400 MHz, $CDCl_3$) 7.49 (td, *J* = 7.5, 2.0 Hz, 1H), 7.24 – 7.16 (m, 1H), 7.11 (td, *J* = 7.5, 1.0 Hz, 1H), 7.00 (ddd, *J* = 10.5, 8.0, 1.0 Hz, 1H), 3.96 (dd, *J* = 10.5, 2.5 Hz, 1H), 3.23 - 3.17 (m, 1H), 2.82 (td, *J* = 11.5, 2.5 Hz, 1H), 1.98 (bs, 1H), 1.92 – 1.78 (m, 2H), 1.72 – 1.62 (m, 1H), 1.62 – 1.43 (m, 3H); **^{13}C NMR** δ_C (100 MHz, $CDCl_3$) 160.3 (d, *J* = 245.0 Hz),

132.1 (d, *J* = 13.0 Hz), 128.3 (d, *J* = 8.5 Hz), 127.8 (d, *J* = 4.5 Hz), 124.4 (d, *J* = 3.5 Hz), 115.3 (d, *J* = 22.0 Hz), 54.9 (d, *J* = 2.5 Hz), 47.9, 33.5, 26.0, 25.4; **IR** υ_{max}/cm^{-1} 3333 (N-H), 2977 (C-H), 2853 (C-H); **HRMS** calcd. for $C_{11}H_{15}N$ 180.1189 [$M+H^+$], found 180.1279.

S4.3. General procedure for the preparation of iminium ions (15a-15d, 17).

General route to iminium halide salts.

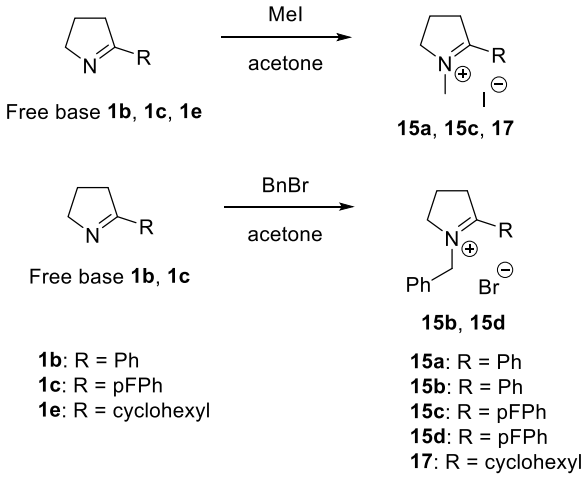

The free base imines **1b**, **1c** and **1e** were prepared as previously described (1, 2) without subsequent formation of the hydrochloride salts. To a solution of the free base imine **1b**, **1c** or **1e** (1 equiv.) in acetone (2 mL/mmol) was added alkyl iodide (methyl iodide or benzyl bromide, 6 equiv.) and stirred at room temperature overnight. The precipitate formed was isolated by filtration, washed with diethyl ether and dried under vacuum to afford the iminium halide salt. For products that were soluble in acetone, addition of diethyl ether caused precipitation and allowed for subsequent isolation by filtration.

1-Methyl-5-phenyl-3,4-dihydro-2*H*-pyrrol-1-ium iodide (15a)

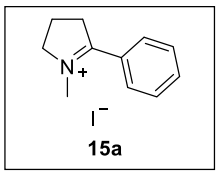

15a

Free base **1b** (100 mg, 0.69 mmol) was subjected to the general method above. Addition of diethyl ether after the reaction caused formation of an insoluble yellow oil. The solvent was decanted and the oil washed with cold acetone diethyl ether and dried under vacuum to afford **15a** as a yellow oil which solidified (57 mg, 0.20 mmol, 29%).

^{1}H NMR δ_H (400 MHz, $CDCl_3$) 7.84 (m, 2H,), 7.62 (m, 1H,), 7.53 (m, 2H,), 4.60 (t, J = 7.8 Hz, 2H), 3.71 (m, 2H), 3.65 (s, 3H), 2.49 (app quint, J = 8.0 Hz, 2H); **^{13}C NMR** δ_C (100 MHz CD_3OD) 187.6, 135.5, 130.7, 130.6, 128.4, 65.0, 41.5, 40.1, 19.5; **IR** ν_{max}/cm^{-1} 2932 (C-H), 1657 (C=N), 1597 (C=C), 1575 (C=C); **MS** m/z 254 [M^+], 160.2 [M^+]; **HRMS** calcd. for $C_{11}H_{14}N$ 160.1126 [$M]^+$, found 160.1120.

1-Benzyl-5-phenyl-3,4-dihydro-2*H*-pyrrol-1-ium bromide (15b)

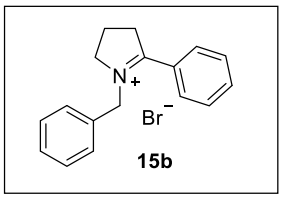

15b

Free base **1b** (100 mg, 0.69 mmol) afforded **15b** as an off-white solid (195 mg, 0.61 mmol, 89%). **^{1}H NMR** δ_H (400 MHz, $CDCl_3$) 7.94 (m, 2H), 7.63 (m, 2H), 7.56 (m, 1H), 7.47-7.37 (m, 5H), 4.16 (s, 2H), 3.22 (app t, J = 6.6 Hz, 2H), 3.04 (m, 2H), 2.31 (m, 2H); **^{13}C NMR** δ_C (100 MHz CD_3OD) 189.9, 135.6, 132.8, 130.9, 130.7, 130.6, 130.0, 129.8, 128.5, 62.1, 56.6, 42.3, 19.6; **IR** ν_{max}/cm^{-1} 2922 (C-H), 2776 (C-H), 1681 (C=N)1449 (C=C); **MS** m/z 236 [M^+]; **HRMS** calcd. for $C_{17}H_{18}N$ 236.1439 [M^+], found 236.1443.

5-(4-Fluorophenyl)-1-methyl-3,4-dihydro-2*H*-pyrrol-1-ium iodide (15c)

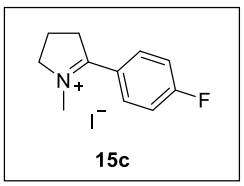

15c

Free base **1c** (125 mg, 0.77 mmol) afforded **15c** as a pale yellow solid (88 mg, 0.29 mmol, 37%). **^{1}H NMR** δ_H (400 MHz, $CDCl_3$) 7.97 (m, 2H), 7.29 (m, 2H), 4.62 (t, *J* = 7.8 Hz, 2H), 3.76 (m, 2H), 3.70 (s, 3H), 2.54 (app quin, *J* = 8.0 Hz, 2H); **^{13}C NMR** δ_C (100 MHz CD_3OD) 186.3, 167.4 (d, *J* = 256.9 Hz), 134.2 (d, *J* = 10.1 Hz), 124.7 (d, *J* = 3.2 Hz), 117.9 (d, *J* = 22.5 Hz), 65.2, 41.6, 40.2, 19.5; **IR** ν_{max}/cm^{-1} 2960 (C-H), 2934 (C-H), 1671 (C=N), 1594 (C=C), 1508 (C=C); **MS** *m*/*z* 178 [M^+]; **HRMS** calcd. for $C_{11}H_{13}NF$ 178.1027 [M^+], found 178.1035.

1-Benzyl-5-(4-fluorophenyl)-3,4-dihydro-2*H*-pyrrol-1-ium bromide (15d)

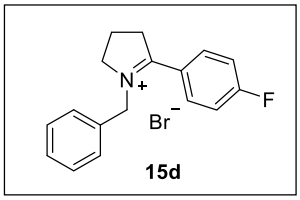

15d

Free base **1c** (125 mg, 0.77 mmol) afforded **15d** as a white solid (172 mg, 0.61 mmol, 79%). **^{1}H NMR** δ_H (400 MHz, $CDCl_3$) 7.98 (m, 2H), 7.62 (m, 2H), 7.39 (m, 3H), 7.11 (m, 2H), 4.14 (s, 2H), 3.21 (t, *J* = 6.8 Hz, 2H), 3.02 (m, 2H), 2.30 (m, 2H); **^{13}C NMR** δ_C (100 MHz CD_3OD) 188.7, 166.3 (d, *J* = 257.4 Hz), 132.8, 130.7, 133.6 (d, *J* = 9.7 Hz), 130.6, 129.8, 124.8 (d, *J* = 3.2 Hz), 118.1 (d, *J* = 22.5 Hz), 62.2, 56.7, 42.2, 19.6; **IR** ν_{max}/cm^{-1} 2901 (C-H), 2758 (C-H), 1682 (C=N); 1594 (C=C), 1505 (C=C); **MS** *m*/*z* 254 [M^+]; **HRMS** calcd. for $C_{17}H_{17}NF$ 254.1340 [M^+], found 254.1329.

5-Cyclohexyl-1-methyl-3,4-dihydro-2*H*-pyrrol-1-ium iodide (17)

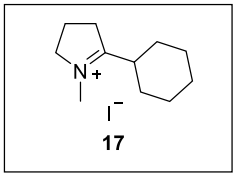

17

Free base **1e** (190 mg, 1.26 mmol) afforded **17** as a pale yellow solid (265 mg, 0.90 mmol, 72%). **^{1}H NMR** δ_H (400 MHz, $CDCl_3$) 4.40-4.36 (m, 2H), 3.59 (s, 3H), 3.38-3.34 (m, 2H), 2.92-2.85 (m, 1H), 2.36-2.39 (m, 2H), 2.19-2.10 (m, 2H), 1.92-1.78 (m, 3H), 1.45-1.20 (m, 5H); **^{13}C NMR** δ_C (100 MHz CD_3OD) 197.3, 64.0, 41.0, 37.8, 29.9, 26.4, 26.1, 19.0, 18.9; **IR** ν_{max}/cm^{-1} 2921 (C-H), 2852 (C-H), 1676 (C=N); **MS** *m*/*z* 166 [M^+]; **HRMS** calcd. for $C_{11}H_{20}N$ 166.1590 [M^+], found 166.1586.

S4. 4. Procedure for the preparation of tertiary amines (16a-16d, 18)

To a solution of *N*-Alkyliminium halide in methanol at 0°C was added $NaBH_4$ (2 equiv.) and the reaction stirred at room temperature for 1 h. The reaction was quenched with 3 M HCl until pH 1 and left to stir for 15 mins. The pH was adjusted to pH 14 by the addition of 10 M NaOH and the product extracted into CH_2Cl_2. The organic phase was dried over $MgSO_4$ and the solvent removed under reduced pressure to the give product amine.

1-Methyl-2-phenylpyrrolidine (16a)

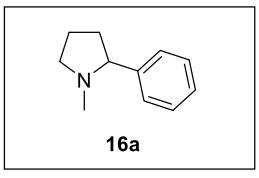

16a

Following the general procedure, iminium halide **15a** (50 mg, 0.17 mmol) afforded **(±)-16a** (22 mg, 0.14 mmol, 82%) as a pale colourless oil. **^{1}H NMR** δ_H (400 MHz, $CDCl_3$) 7.38-7.30 (m, 4H), 7.27-7.22 (m, 1H), 3.26 (m, 1H), 3.04 (t, *J* = 8.0 Hz, 1H), 2.34-2.24 (m, 1H), 2.21-2.24 (m, 1H), 2.18 (s, 3H), 2.02-1.90 (m, 1H,), 1.86-1.72 (m, 2H); **^{13}C NMR** δ_C (100 MHz $CDCl_3$) 143.2, 128.3, 127.5, 127.0, 71.7, 57.1, 40.5, 35.1, 22.5; **MS** *m*/*z* 162 [M+H^+]; **HRMS** calcd. for $C_{11}H_{15}N$ 162.1277 [M+H^+], found 162.1280.

1-Benzyl-2-phenylpyrrolidine (16b)

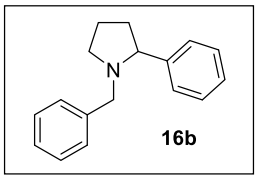

Following the general procedure, iminium halide **15b** (50 mg, 0.16 mmol) afforded **(±)-16b** (19 mg, 0.8 mmol, 51%) as a pale yellow oil after column chromatography (silica, 10% v/v ethyl acetate-cyclohexane + 0.1% triethylamine). **^{1}H NMR** δ_H (400 MHz, $CDCl_3$) 7.50-7.46 (m, 2H), 7.39-7.33 (m, 2H), 7.31-7.19 (m, 6H), 3.86 (d, *J* = 13.0 Hz, 1H), 3.37 (t, *J* = 8.0 Hz, 1H), 3.10 (m, 1H), 3.04 (d, *J* = 13.0 Hz, 1H), 2.25-2.14 (m, 2H), 1.94-1.84 (m, 1H), 1.84-1.68 (m, 2H); **^{13}C NMR** δ_C (100 MHz $CDCl_3$) 143.9, 139.8, 128.7, 128.4, 128.1, 127.5, 127.0, 126.6, 69.6, 58.1, 53.3, 35.2, 22.3; **MS** *m*/*z* 238 [M+H$^+$]; **HRMS** calcd. for $C_{17}H_{19}N$ 238.1590 [M+H$^+$], found 238.1589.

2-(4-Fluorophenyl)-1-methylpyrrolidine (16c)

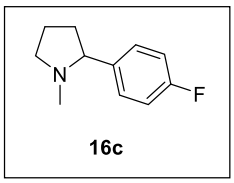

Following the general procedure, iminium halide **15c** (50 mg, 0.16 mmol) afforded **(±)-16c** (27 mg, 0.15 mmol, 93%) as a pale yellow oil. **^{1}H NMR** δ_H (400 MHz, $CDCl_3$) 7.33-7.28 (m, 2H), 7.04-6.98 (m, 2H), 3.26-3.21 (m, 1H), 3.04-3.00 (m, 1H), 2.35-2.32 (m, 1H) 2.20-2.12 (m, 1H), 2.16 (s, 3H), 2.01-1.89 (m, 1H), 1.85-1.66 (m, 2H); **^{13}C NMR** δ_C (100 MHz $CDCl_3$) 161.9 (d, *J* = 245 Hz), 138.8 (d, *J* = 2.8 Hz), 128.9 (d, *J* = 7.8 Hz), 115.1 (d, *J* = 21.6 Hz), 70.9, 57.0, 40.4, 35.2, 22.4. Data consistent with literature values (*3*).

1-Benzyl-2-(4-fluorophenyl)pyrrolidine (16d)

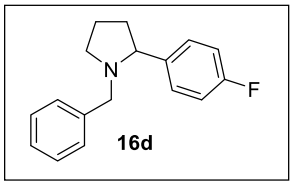

Following the general procedure, iminium halide **15d** (23 mg, 0.07 mmol) afforded **(±)-16d** (9 mg, 0.04 mmol, 51%) as a pale yellow oil after column chromatography (silica, 10% v/v ethyl acetate-cyclohexane + 0.1% triethylamine). **^{1}H NMR** δ_H (400 MHz, $CDCl_3$) 7.46-7.40 (m, 2H), 7.32-7.19 (m, 5H), 7.07-6.99 (m, 2H), 3.81 (d, *J* = 13.0 Hz, 1H), 3.25 (t, *J* = 8.0 Hz, 1H), 3.09 (m, 1H), 3.04 (d, *J* = 13.0 Hz, 1H), 2.25-2.12 (m, 2H), 1.95-1.82 (m, 1H), 1.82-1.65 (m, 2H); **^{13}C NMR** δ_C (100 MHz $CDCl_3$) 161.9 (d, *J* = 245.0 Hz), 139.6, 128.9 (d, *J* = 8.0 Hz), 128.6, 128.1, 126.7, 115.2 (d, *J* = 21.0 Hz), 68.9, 58.0, 53.3, 35.3, 22.3; **MS** *m*/*z* 256 [M+H$^+$]; **HRMS** calcd. for $C_{17}H_{18}NF$ 256.1496 [M+H$^+$], found 256.1500.

2-Cyclohexyl-1-methylpyrrolidine (18)

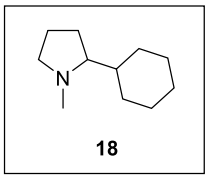

Iminium halide **17** (50 mg, 0.17 mmol) afforded **(±)-18** (24 mg, 0.14 mmol, 84%) as a pale yellow oil. **^{1}H NMR** δ_H (400 MHz, $CDCl_3$) 3.08-3.02 (m, 1H), 2.28 (s, 3H), 2.14-2.08 (m, 1H), 1.97-1.92 (m, 1H), 1.79-1.55 (m, 9H), 1.54-1.44 (m, 1H), 1.31-1.07 (m, 3H), 1.05-0.94 (m, 2H); **^{13}C NMR** δ_C (100 MHz $CDCl_3$) 70.9, 57.7, 41.2, 39.3, 31.2, 27.0, 26.9, 26.4, 26.2, 26.0, 22.4.

S4.5. Preparation of 2-methyl-3,4-dihydroisoquinolin-2-ium triflate (19a)

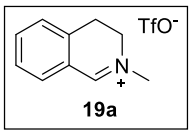

To a solution of 3,4-dihydroisoquinoline **7** (158 mg, 1.20 mmol) in CH_2Cl_2 (2 mL), methyl triflate (143 µL, 1.26 mmol) was added and the solution stirred at room temperature for 1.5 hours. After removal of the solvent, pentane (5 mL) was added. The solid was filtrated, washed with pentane (2 mL) and dried to give **19a** (306 mg, 86% yield) as a pale yellow solid. **^{1}H NMR** δ_H (400 MHz, $CDCl_3$) 9.08 (s, 1H), 7.86-7.78 (m,

2H), 7.60-7.49 (m, 2H), 4.11 (t, *J* = 8.1 Hz, 2H), 3.83 (s, 3H), 3.33 (t, *J* = 8.1 Hz, 2H); **^{13}C NMR** δ_C (100 MHz, CD_3OD) 168.6, 139.2, 137.6, 134.7, 129.5, 126.1, 123.4, 120.3, 51.2, 48.1, 25.9.

S4. 6. Preparation of 1,2-dimethyl-3,4-dihydroisoquinolin-2-ium iodide (19b)

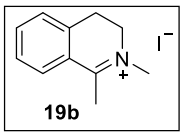

19b

To a stirred solution of 1-methyl-3,4-dihydroisoquinoline hydrochloride **9** (100 mg, 0.550 mmol) in acetonitrile (2 mL) was added methyl iodide (205 µL, 3.30 mmol). After the reaction had gone to completion, the precipitate was filtered and washed with acetone and left to dry in air to afford 1,2-dimethyl-3,4-dihydroisoquinolin-2-ium iodide **19b** (68 mg, 43% yield) as a bright yellow solid. **^{1}H NMR** δ_H (400 MHz, $CDCl_3$) 7.88 (d, *J* = 8.1 Hz, 1H), 7.68 (td, *J* = 7.6, 1.1 Hz, 1H), 7.52 – 7.47 (m, 1H), 7.36 (d, *J* = 7.6 Hz, 1H), 4.20 (t, *J* = 7.6 Hz, 2H), 3.98 (s, 3H), 3.39 (t, *J* = 7.6 Hz, 2H), 3.01 (s, 3H); **^{13}C NMR** δ_C (100 MHz, $CDCl_3$) 176.1, 136.3, 136.2, 130.1, 128.3, 128.2, 127.3, 53.5, 47.2, 25.8, 20.7

S4.7. Preparation of standard sample of 2-methyl-1,2,3,4-tetrahydroisoquinoline (20a)

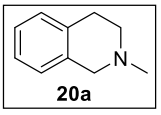

20a

To a solution of iminium ion **19a** (100 mg, 0.34 mmol) in MeOH (5 mL) was added $NaBH_4$ (13 mg, 0.34 mmol) at 0˚C under nitrogen atmosphere. The solution was stirred for 1 hour at room temperature. Water (20 mL) and CH_2Cl_2 (25 mL) were added, the two phases separated and the aqueous phase extracted with CH_2Cl_2 (25 mL). The combined organic phases were dried over $MgSO_4$ and concentrated under vacuum to give **20a** (47 mg, 95% yield) as a white solid. **^{1}H NMR** δ_H (400 MHz, $CDCl_3$) 7.21-7.01 (m, 4H), 3.63 (s, 2H), 2.96 (t, *J* = 6.0 Hz, 2H), 2.73 (t, *J* = 6.0 Hz, 2H), 2.49 (s, 3H); **^{13}C NMR** δ_C (100 MHz, $CDCl_3$) 100 MHz, $CDCl_3$ δ: 134.5, 133.7, 128.7, 126.4, 126.0, 125.6, 57.9, 52.9, 46.0, 29.1.

S4. 8. Preparation of standard solution of 2-substituted cyclic amine 20b

1,2-dimethyl-1,2,3,4-tetrahydroisoquinoline (20b): 19b (30 mg, 0.104 mmol) was

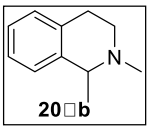

dissolved in dH_2O:MeOH (1:4, 5 mL) and was reduced by addition of $NaBH_4$ (4 mg, 0.104 mmol). The reaction was quenched and then basified as previously described before being extracted into diethyl ether (3 x 15 mL). Subsequently, the organic layers were combined and dried over $MgSO_4$. The solvent was then carefully removed on a rotary evaporator at 35°C and 300 mbar pressure to yield tertiary amine **20b** (15 mg, 89% yield) as a brown oil. ^{1}H NMR δ_H (400 MHz, $CDCl_3$) 7.17 – 7.06 (m, 4H), 3.61 (q, *J* = 6.6 Hz, 1H), 3.04 (ddd, *J* = 11.6, 6.3, 5.2 Hz, 1H), 2.95 – 2.79 (m, 2H), 2.62 (ddd, *J* = 11.6, 7.2, 4.9 Hz, 1H), 2.49 (s, 3H), 1.40 (d, *J* = 6.6 Hz, 3H); ^{13}C NMR (100 MHz, $CDCl_3$) δ: 140.0, 134.1, 128.8, 127.0, 125.9, 125.9, 59.2, 49.2, 43.2, 28.4, 19.8.

Section S5. Analysis: Chromatography columns, conditions and retention times for investigated substrates.

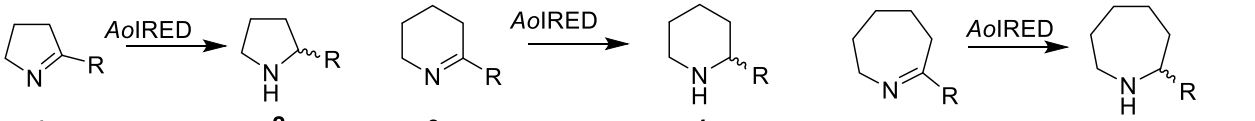

1a: R= Me
1b: R=Ph
1c: R= pFPh
1d: R= p-OMePh

2a: R= Me
2b: R=Ph
2c: R= pFPh
2d:R= p-OMePh

3a: R= Me
3b: R=Ph
3c: R= pFPh
3d: R= p-OMePh
3e: R= m-FPh
3f: R= o-FPh
3g: Propyl

4a: R= Me
4b: R=Ph
4c: R= pFPh
4d: R= p-OMePh
4e: R= m-FPh
4f: R= o-FPh
4g: R= Propyl

5a: R= Me
5b: R=p-OMePh

6a: R= Me
6b: R=p-OMePh

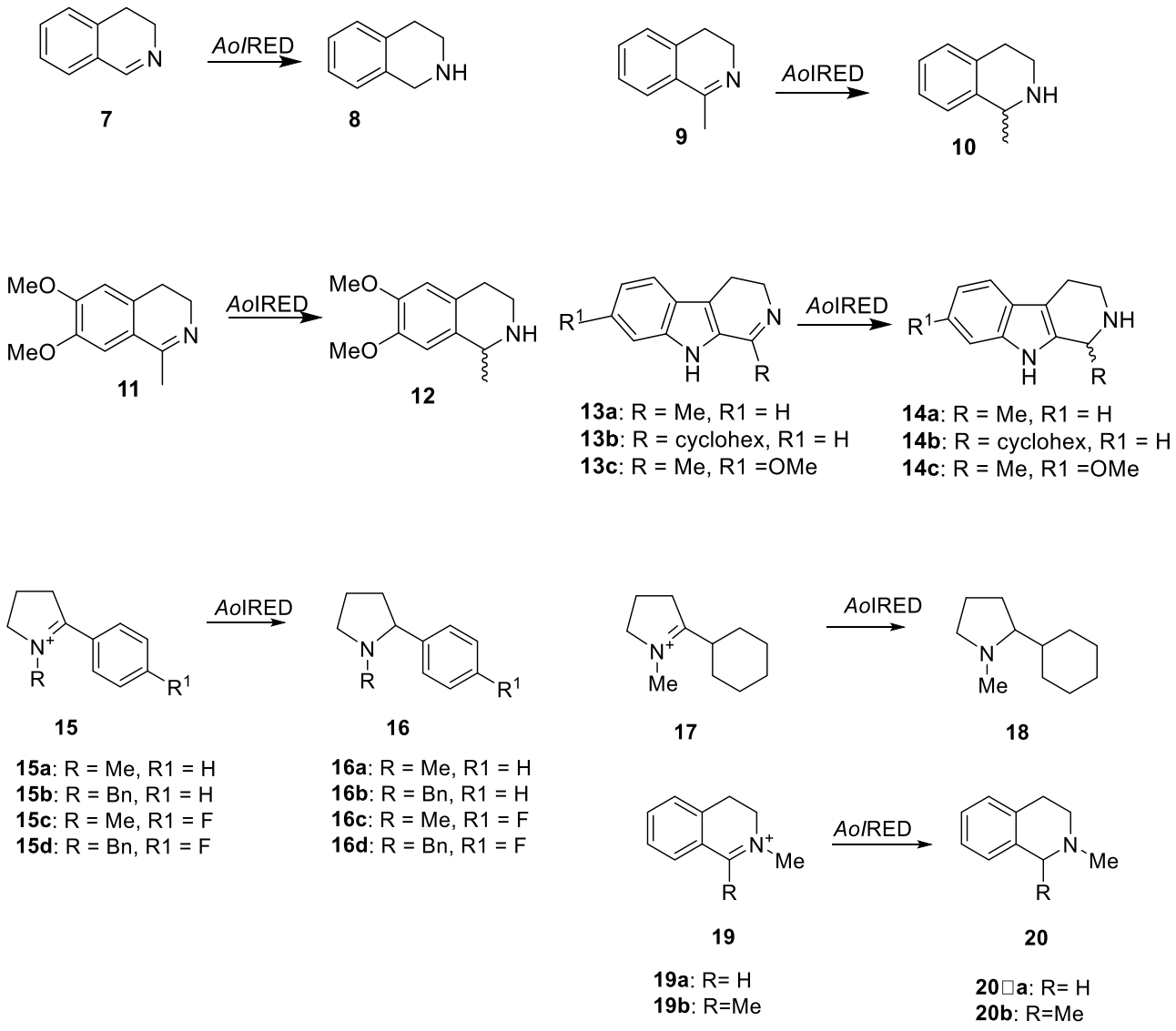

Figure S6. A panel of imines/iminium ions screened against *Ao*IRED.

S5. 1. HPLC and GC analyses: methods and conditions

Imines/ iminion ions and the resulting biotransformation products were analyzed by normal phase chiral HPLC using isocratic methods of different solvents ratio of *n*-hexane and isopropanol, with 0.1% diethylamine as additive. Columns used include: Daicel CHIRALPAK®IA 250 mm × 4.6 mm, 5 μm; Daicel; CHIRALPAK®IC 250 mm × 4.6 mm, 5 μm; Daicel CHIRALPAK®IE 250 mm × 4.6 mm, 5 μm. The flow rate was maintained at 1 mL min^{-1} and elutes were detected by the U.V. detector at a wavelength of 265 nm.

To account for the variation in UV response between imine and amines, the relative response factors were experimentally determined. Correction factors were calculated from the ratio of the slopes of standard curves plotted for varying concentrations of both the imine and amine at a UV detection wavelength of 265 nm.

Table S1. HPLC analysis: Methods and retention times for substrates and biotransformation products

Imine	Amine	Column	*n*-hexane/IPA/ diethylamine running solvent ratio	Relative response factor (A_{imine}/A_{amine})	Imine retention time (min)	Amine retention Time (min)	
						T^1	T^2
1b	**2b**	CHIRALPAK®IC	90:10:0.1	25.3	9.3	7.4 (*R*)	8.02 (*S*)
1c	**2c**	CHIRALPAK®IA	98:2:0.1	4.68	8.7	10.3 (*R*)	11.3 (*S*)
1d	**2d**	CHIRALPAK®IE	90:10:0.1	36.8	15.7	12.4 (*R*)	13.6 (*S*)
3c	**4c**	CHIRALPAK®IC	98:2:0.1	2.53	8.3	5.4 (*R*)	5.8 (*S*)
3d	**4d**	CHIRALPAK®IC	90:10:0.1	19.1	16.1	8.9 (*R*)	12.9 (*S*)
3e	**4e**	CHIRALPAK®IC	98:2:0.1	1.64	9.5	5.6 (*R*)	6.3 (*S*)
3f	**4f**	CHIRALPAK®IC	98:2:0.1	1.29	11.9	6.0 (*S*)	7.3 (*R*)
5b[b]	**6b**	CHIRALPAK®IC	90:10:0.1	21.4	17.8	7.5	10.5
7	**8**	CHIRALPAK®IC	90:10:0.1	9.79	14.1	10.6[a]	
9	**10**	CHIRALPAK®IC	97:3:0.1	9.10	19.1	11.1 (*S*)	12.2 *(R*)
11	**12**	CHIRALPAK®OD-H	90:10:0.1	6.43	8.7	12.9 (*S*)	16.7 (*R*)
13a	**14a**	CHIRALPAK®IC	90:10:0.1	0.43	8.6		
13b	**14b**	CHIRALPAK®IC	90:10:0.1	0.314	6.1	10.4 (*S*)	11.4 (*R*)
13c	**14c**	CHIRALPAK®IC	90:10:0.1	1.79	7.2	11.9 (*S*)	14.1 (*S*)
19a	**20a**	CHIRALPAK®IC	90:10:0.1	2.5	5.2	6.8[a]	

[a] Non-chiral product

[b] Absolute configuration undetermined

Table S2. GC analysis: Methods and retention times of substrates and products from biotransformation run on CP-ChiraSil-DEX CB column using derivatised samples.

Compound		Injector temp.	Helium flow/ mL min^{-1}	Oven temp.	Detector temp.	Imine retention time/ min	Amine retention time/ min	
							T^1	T^2
1a	**2a**	200	1.2	90°C - 160°C, 0.5°C min^{-1}, hold 160°C for 10 minutes	250	27.3	29.8 (*R*)	30.5 (*S*)
3a	**4a**	200°C	1.5	50°C - 200°C, 10°C min^{-1}	250°C	10.70	10.8 (*R*)	10.9 (*S*)
5a	**6b**	200°C	1.2	90°C - 160°C, 1°C min^{-1} then 10°C min^{-1} to 200°C	250°C	61.3	35.8 (*S*)	36.2 (*R*)
3b	**4b**	200°C	1.2	90°C - 200°C, 4°C min^{-1}	250°C	18.1	24.8 (*S*)	25.1 (*R*)
3g	**4g**	200°C	1.2	90°C - 200°C, 4°C min^{-1}	250°C	14.9	15.6 (*S*)	15.8 (*R*)
19b	**20b**	200°C	1.2	90°C - 200°C, 4°C min^{-1}	250°C	16.2	12.8 (*R*)	13.2 (*S*)

S5. 2. Conversion of iminium ion substrates 15a-15d and 17.

As the iminium ions are more water soluble compared to other imines due to their charge, an alternative method for determining the conversion was used. A 250 mM stock solution of the iminium halide salt was prepared in DMSO and 10 µL added to the 490 µL biotransformation mixture (total reaction volume 500 µL, 5 mM substrate final concentration) and 10 µL was added to 490 µL of 50 mM $NH_3.BH_3$ in 100 mM sodium phosphate buffer pH 7.5 (total reaction volume 500 µL, 10 equiv. of NH_3BH_3 relative to substrate). Reactions were incubated for 24 h at 30°C. Reactions were worked up by adding 1 mL of CH_2Cl_2 containing decane as internal standard (1 µl decane per 1 mL of CH_2Cl_2) and 10 µL of 10M NaOH. Reactions were vortexed, the organic phase extracted, dried over $MgSO_4$ and immediately analysed by GC-FID. Conversion was determined based on the area of amine product/decane

for the biotransformation relative to the parallel reaction with $NH_3.BH_3$. Reactions were run in triplicate and quoted conversions are averaged values.

Table S3. GC-analysis: Methods and retention times of substrates and products from biotransformation run on CP-ChiraSil-DEX CB column using underivatised samples**.** Absolute configuration was assigned by N-methylation or N-benzylation of pyrrolidine amines (1c,1d, 1e) of known configuration.

Iminium Ion	Amine	Injector temp.	Helium flow/ mL min^{-1}	Oven temp.	Detector temp.	Internal Standard retention time/min (decane)	Amine retention time/ min	
							T^1	T^2
15a	**16a**	200°C	1.2	Hold 100°C for 10 mins, 100°C - 120°C, 2°C min^{-1}, 120°C - 200°C, 20°C min^{-1}.	250°C	3.73	16.49 (*S*)	16.73 (*R*)
15b	**16b**	200°C	1.2	Hold 90°C for 5 mins, 90°C - 160°C, 10°C min^{-1}, hold 160°C for 10 mins, 160°C - 174°C, 2°C min^{-1}, 174°C - 200°C, 20°C min^{-1}.	250°C	5.15	27.81 (*R*)	27.96 (*S*)
15c	**16c**	200°C	1.2	100°C - 111°C, 0.5°C min^{-1}, 111°C – 200 °C, 20°C min^{-1}.	250°C	3.63	19.44 (*S*)	19.69 (*R*)
15d	**16d**	200°C	1.2	Hold 100°C for 5 mins, 100°C - 140°C, 10°C min^{-1}, hold 140°C for 5 mins, 140°C-174°C, 2°C min^{-1}, 174°C - 200°C, 20°C min^{-1}.	250°C	3.72	31.84 (*R*)	31.99 (*S*)
17	**18**	200°C	1.2	50°C - 200°C, 5°C min^{-1}	250°C	9.17	16.93 (*S*)	17.23 (*R*)

S5. 3. Chromatograms

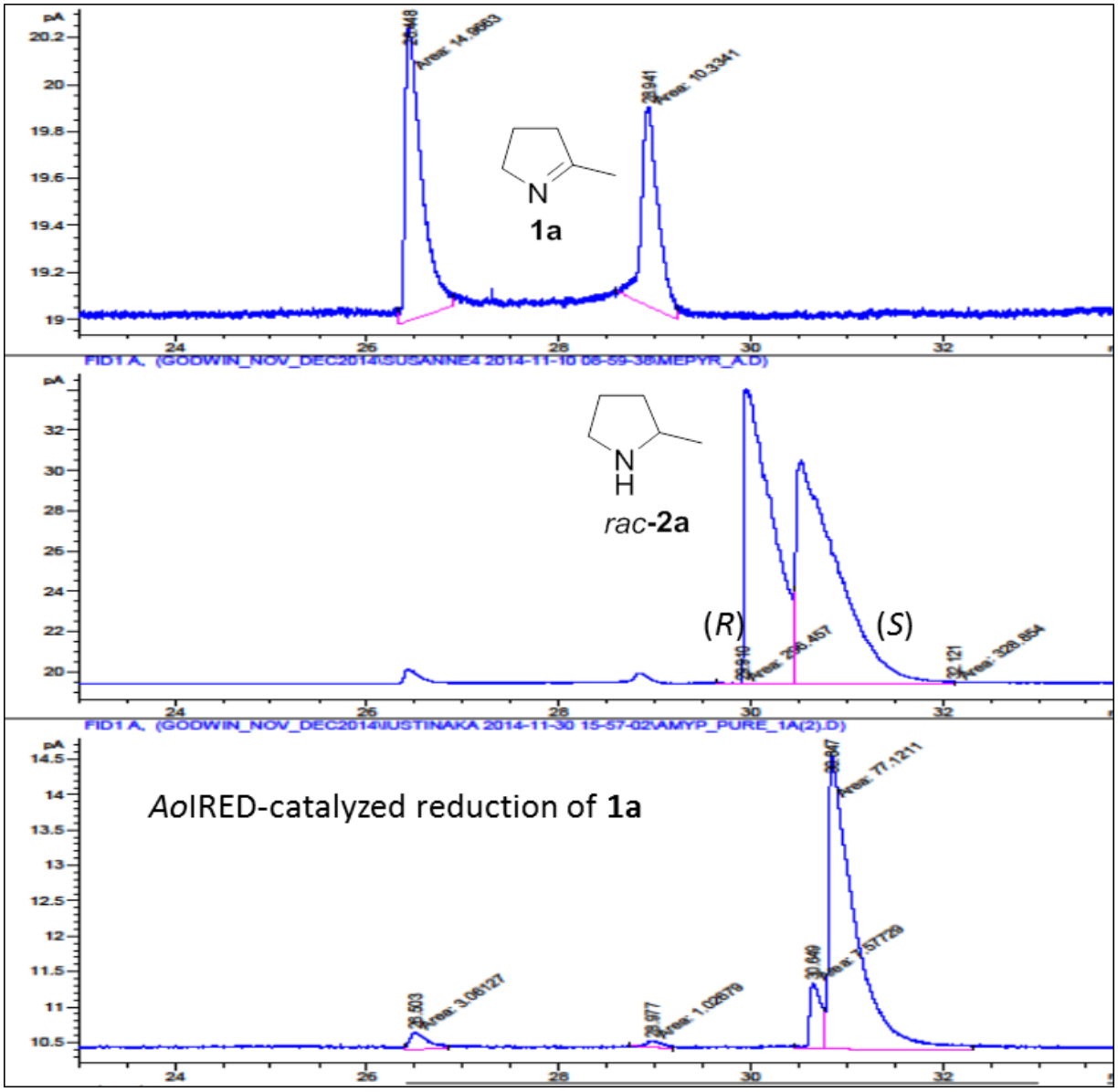

Figure S7. GC-FID analysis chromatogram of *Ao*IRED-catalyzed biotransformation of 2-methyl-1-pyrroline **1a** using CP-ChiraSil-DEX CB column, showing standards of imine **1a** (top) and racemic amine **2a** (middle), followed by biotransformation result (bottom). Note that there are two peaks visible for the imine standard following derivatization; it is assumed that both peaks correspond to the imine substrate.

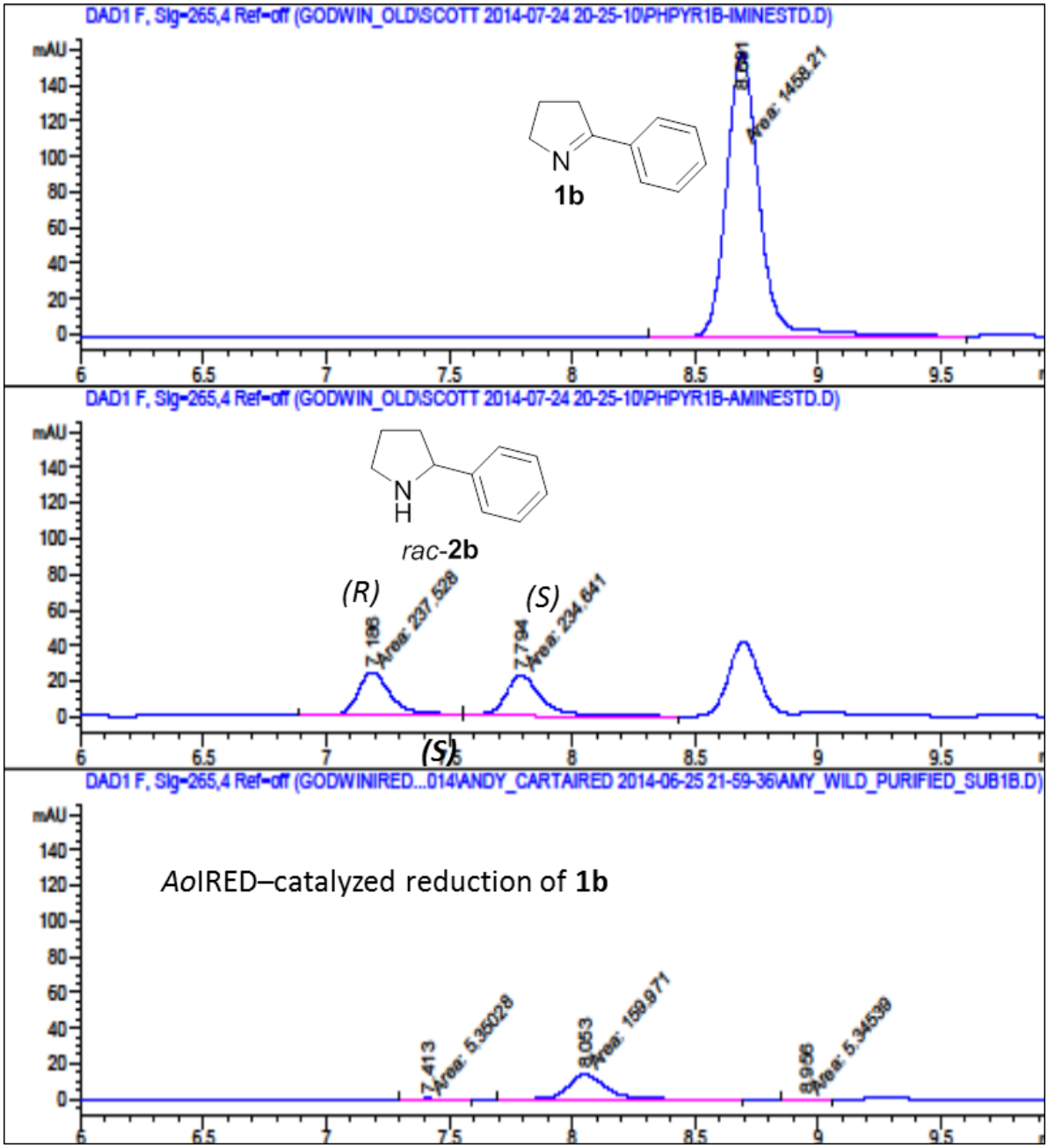

Figure S8. HPLC analysis: chromatogram of *Ao*IRED-catalyzed biotransformation of 2-phenyl-pyrrolidine **1b** using CP-ChiraSil-DEX CB column, showing standards of imine 1b (top) and racemic amine **2b** (middle), followed by biotransformation result (bottom). (Daicel CHIRALPAK®IC 250 mm × 4.6 mm, 5 µm, solvent: hexane/isopropanol/diethylamine = 90/10/0.1, 1 mL/min, 265 nm).

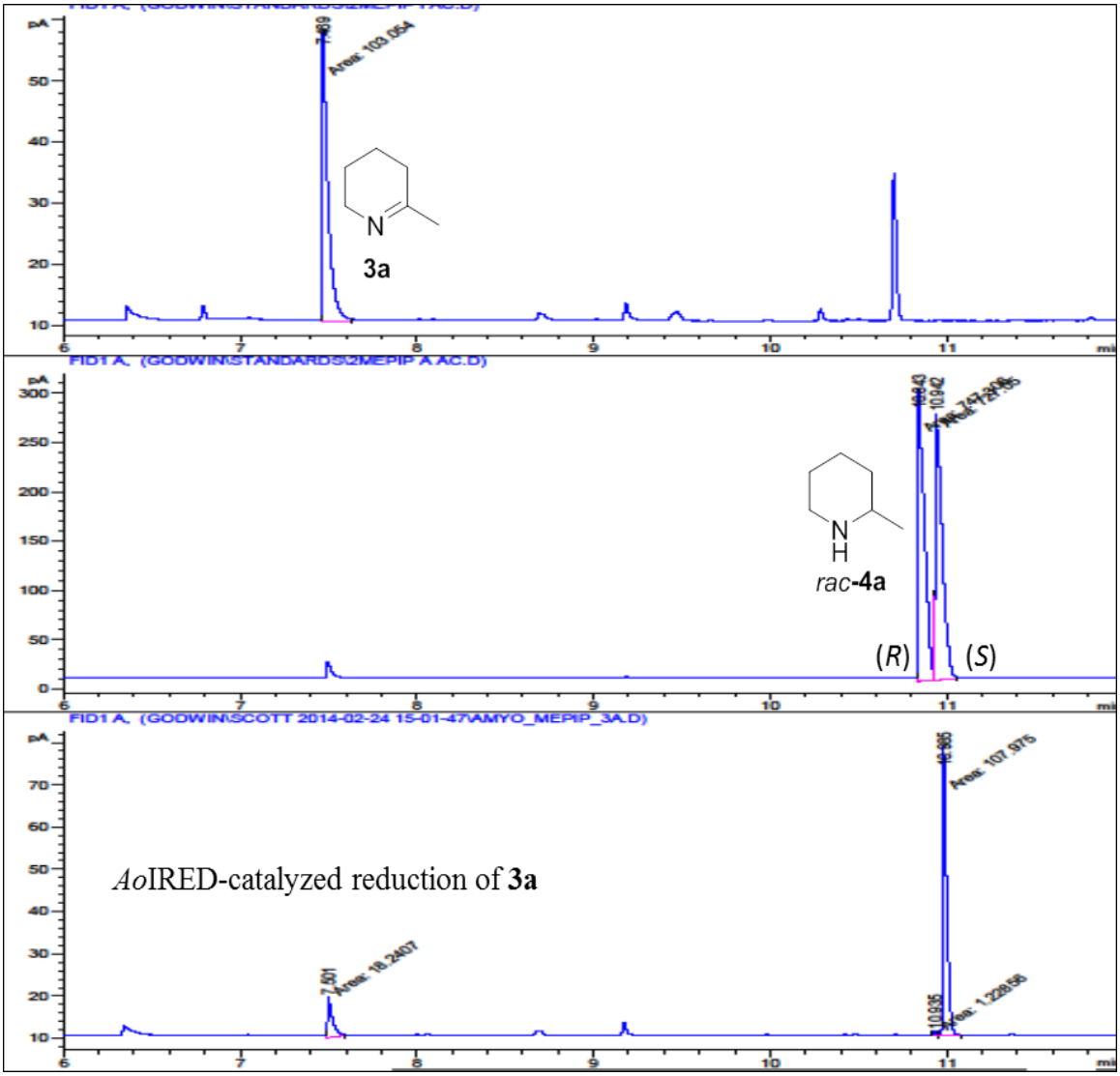

Figure S9a

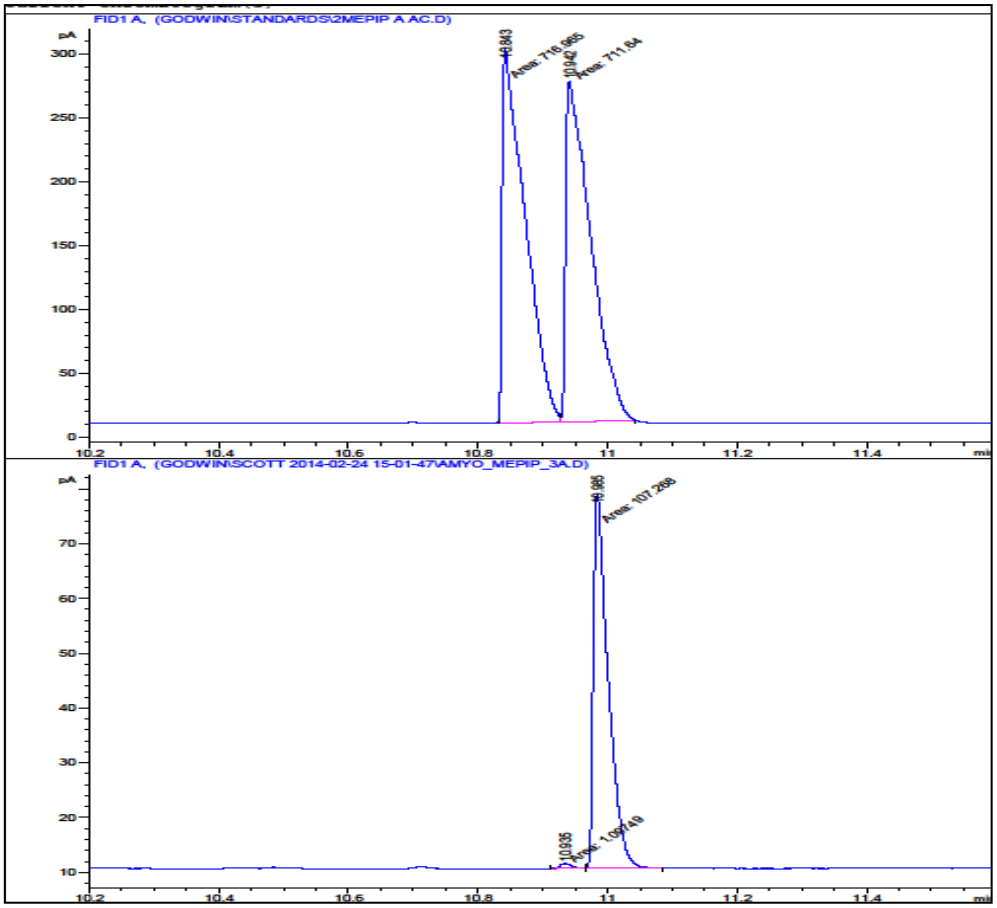

Figure S9b

Figure S9. **S9a:** Chiral GC-FID analysis of *Ao*IRED catalyzed biotransformation of **3a**. Standard solution of **3a** (top), racemic amine standard *rac*-**4a** (middle) and *Ao*IRED-catalyzed biotransformation product (bottom). (Agilent CP-Chirasil-DEX CB column 25 m × 0.25 mm × 0.25 µm). **S9b:** Expansion of separation of enantiomers of **4a** resulting from biotransformation by *Ao*IRED.

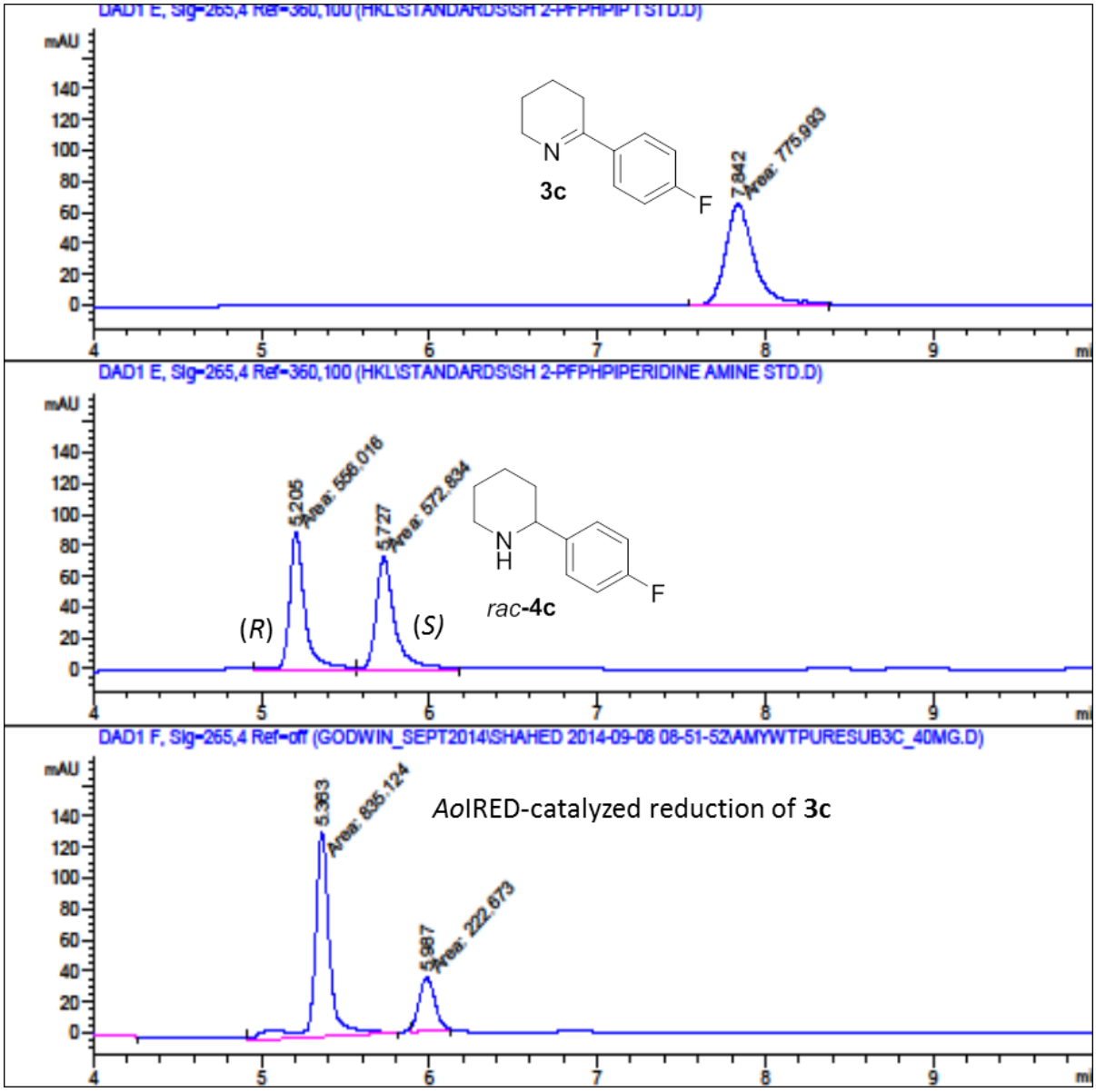

Figure S10. HPLC analysis of *Ao*IRED catalyzed biotransformation of **3c.** Standard solution of **3c** (top), racemic amine *rac*-**4c** (middle) and *Ao*IRED catalyzed biotransformation product (bottom). (Daicel CHIRALPAK®IC 250 mm × 4.6 mm, 5 µm, solvent: hexane/isopropanol/diethylamine = 98/2/0.1, 1 mL/min, 265 nm).

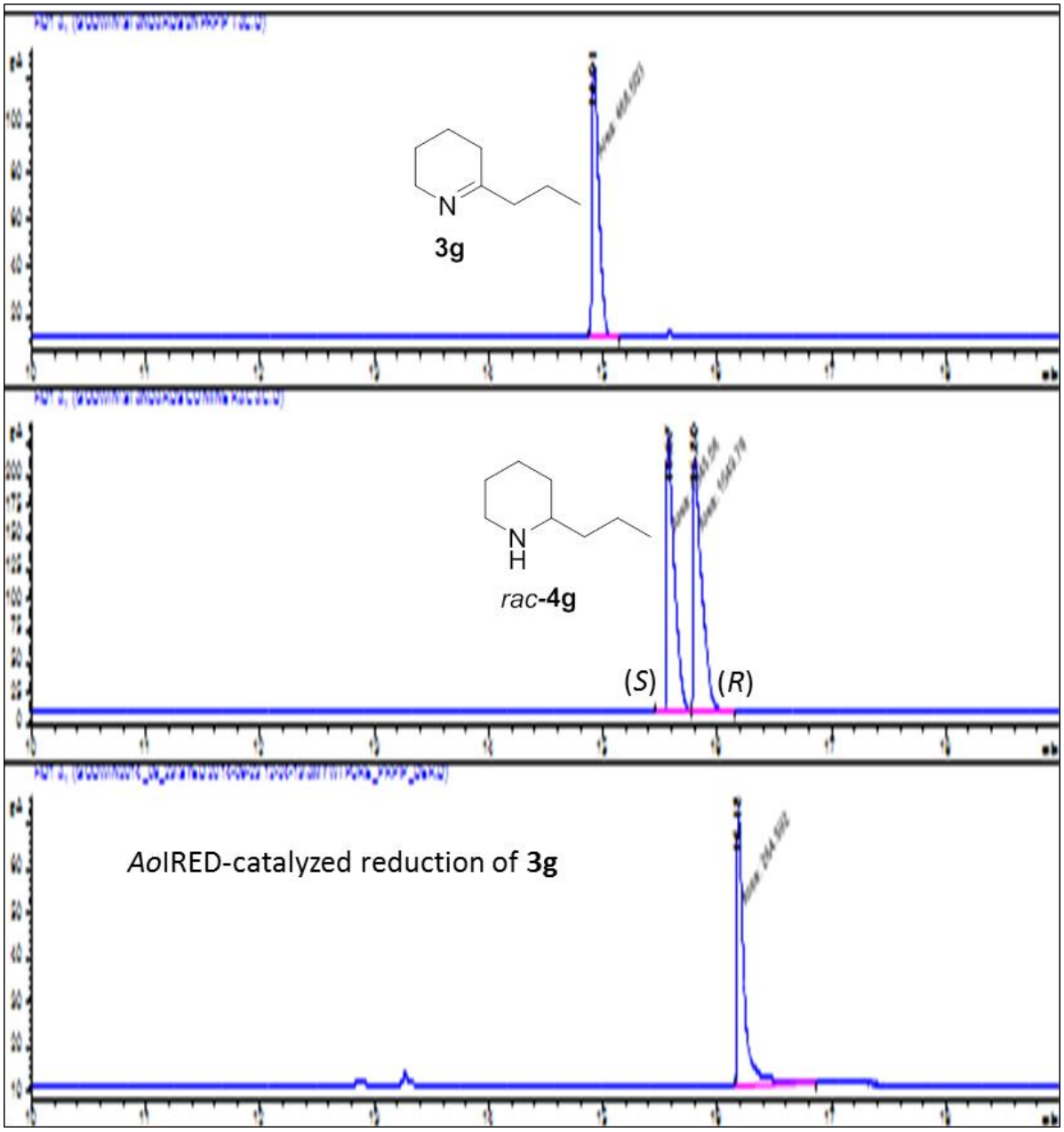

Figure S11. Chiral GC-FID analysis of *Ao*IRED catalyzed biotransformation of **3g**. Standard solution of **3g** (top), racemic amine **4g** standard *rac-4a* (middle) and *Ao*IRED catalysed biotransformation product (bottom). (Agilent CP-Chirasil-DEX CB column 25 m × 0.25 mm).

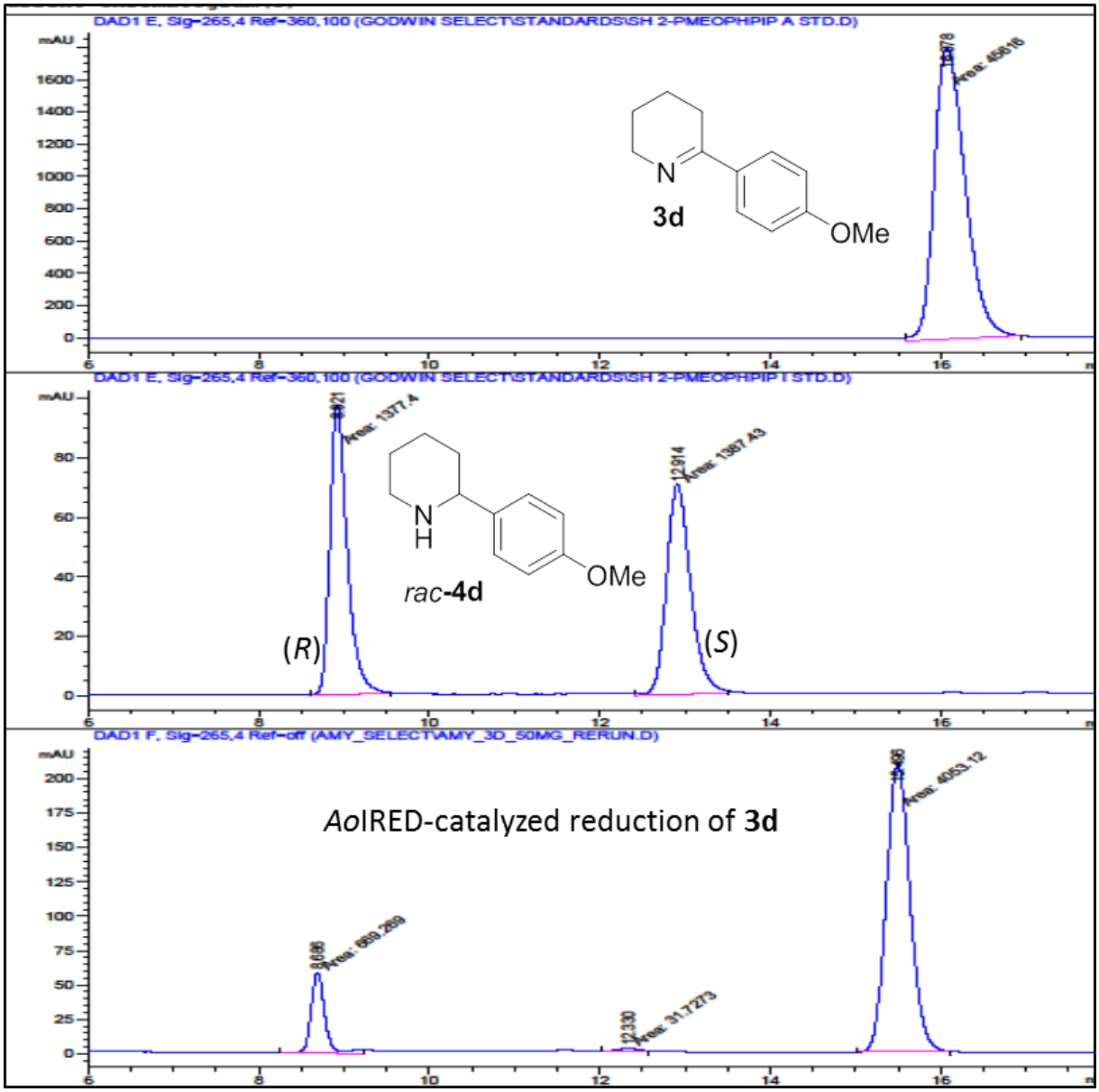

Figure S12 HPLC analysis of *Ao*IRED catalyzed biotransformation of **3d.** Standard solution of **3d** (top), racemic amine **4d** (middle] and *Ao*IRED catalysed biotransformation product (bottom). (Daicel CHIRALPAK®IC 250 mm × 4.6 mm, 5 µm, solvent: hexane/isopropanol/diethylamine = 90/10/0.1, 1 mL/min, 265 nm).

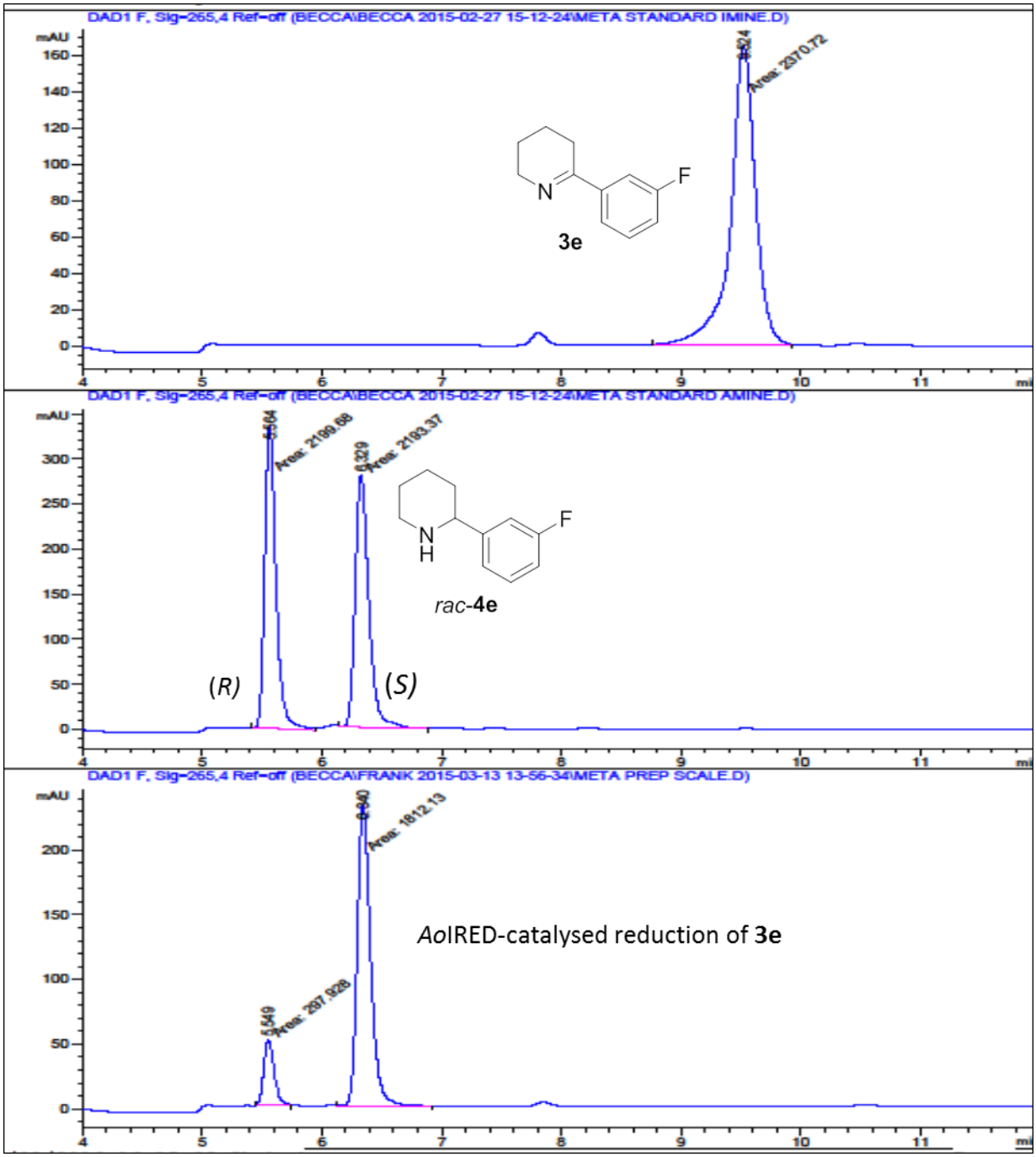

Figure S13. HPLC analysis of *Ao*IRED catalyzed biotransformation of **3e.** Standard solution of **3e** (top), racemic amine **4e** (middle] and *Ao*IRED catalysed biotransformation product (bottom). (Daicel CHIRALPAK®IC 250 mm × 4.6 mm, 5 µm, solvent: hexane/isopropanol/diethylamine = 98/2/0.1, 1 mL/min, 265 nm)

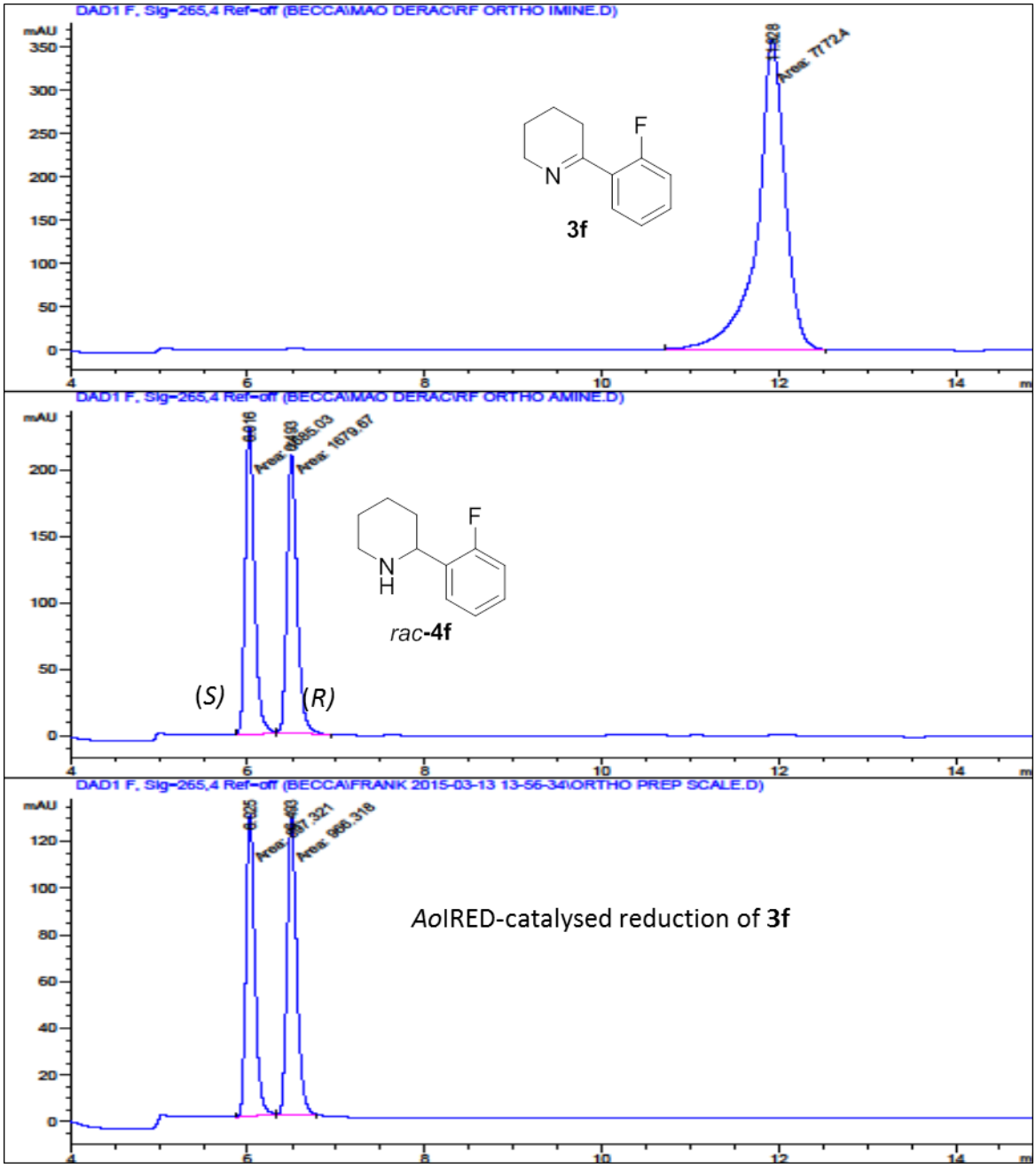

Figure S14. HPLC analysis of *Ao*IRED catalyzed biotransformation of **3f.** Standard solution of **3f** (top), racemic amine **4f** (middle] and *Ao*IRED catalysed biotransformation product (bottom). (Daicel CHIRALPAK®IC 250 mm × 4.6 mm, 5 µm, solvent: hexane/isopropanol/diethylamine = 98/2/0.1, 1 mL/min, 265 nm)

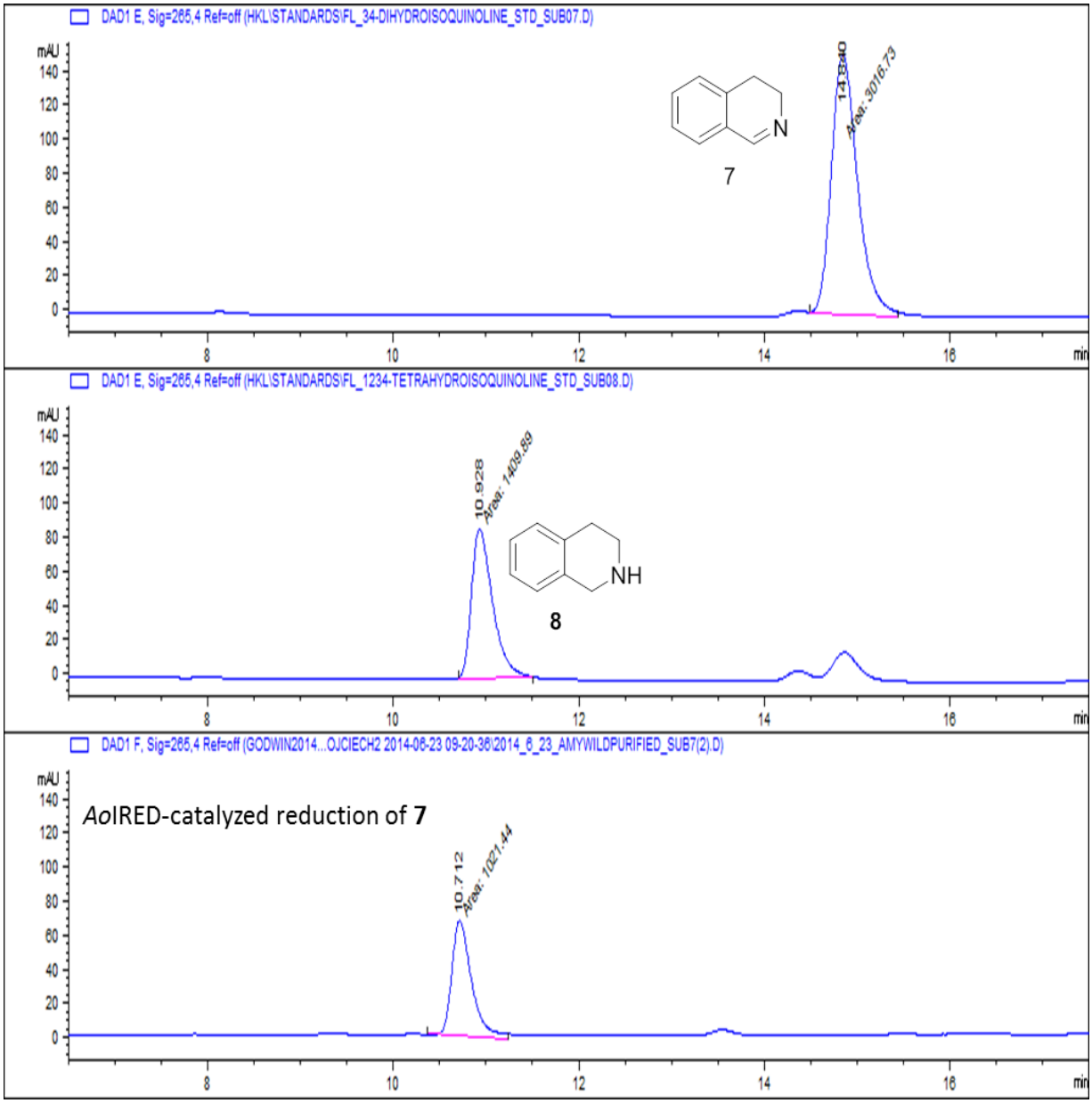

Figure S15. HPLC analysis of *Ao*IRED catalyzed biotransformation of **7.** Standard solution of **7** (top), amine **8** (middle] and *Ao*IRED catalyzed biotransformation product (bottom). (Daicel CHIRALPAK®IC 250 mm × 4.6 mm, 5 µm, solvent: hexane/isopropanol/diethylamine = 90/10/0.1, 1 mL/min, 265 nm).

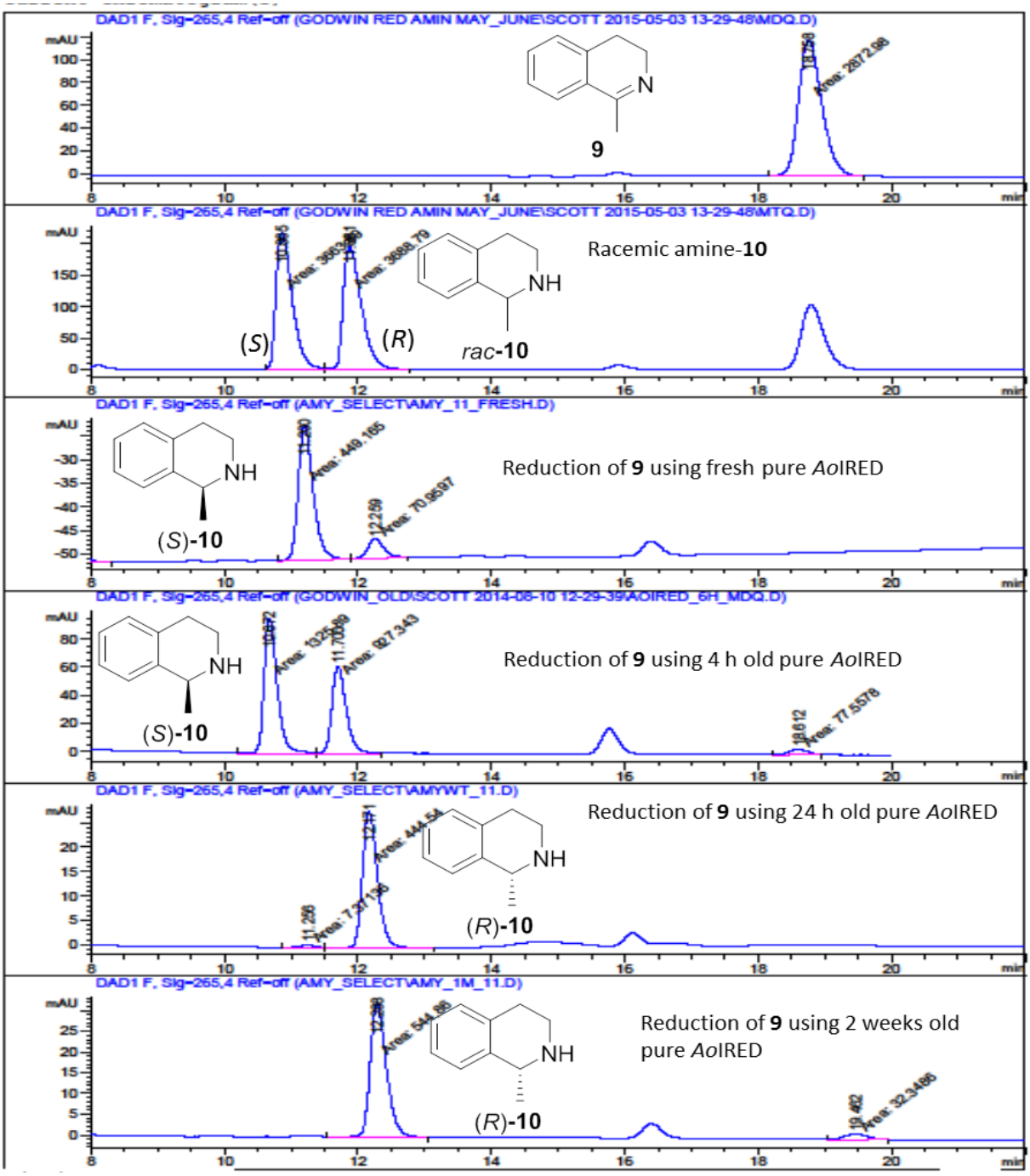

Figure S16. HPLC analysis of *Ao*IRED catalyzed biotransformation of **9**. (Daicel CHIRALPAK®IC 250 mm × 4.6 mm, 5 µm, solvent: hexane/isopropanol/diethylamine = 97/03/0.1, 1 mL/min, 265 nm).

From the top, row 1= standard solution of imine **9**, row 2= standard solution of racemic amine **10**, row 3 =product of biotransformation of 9 using fresh pure *Ao*IRED; row 4= product of biotransformation of 9 using 4 h old pure *Ao*IRED; row 5= product of biotransformation of **9** using 24 h old pure *Ao*IRED; row 6= product of biotransformation of **9** 2 week old pure *Ao*IRED. *Ao*IRED was stored at 4°C and biotransformation mixtures were incubated at 30°C. Note the gradual but complete inversion of selectivity of *Ao*IRED on **9** upon storage.

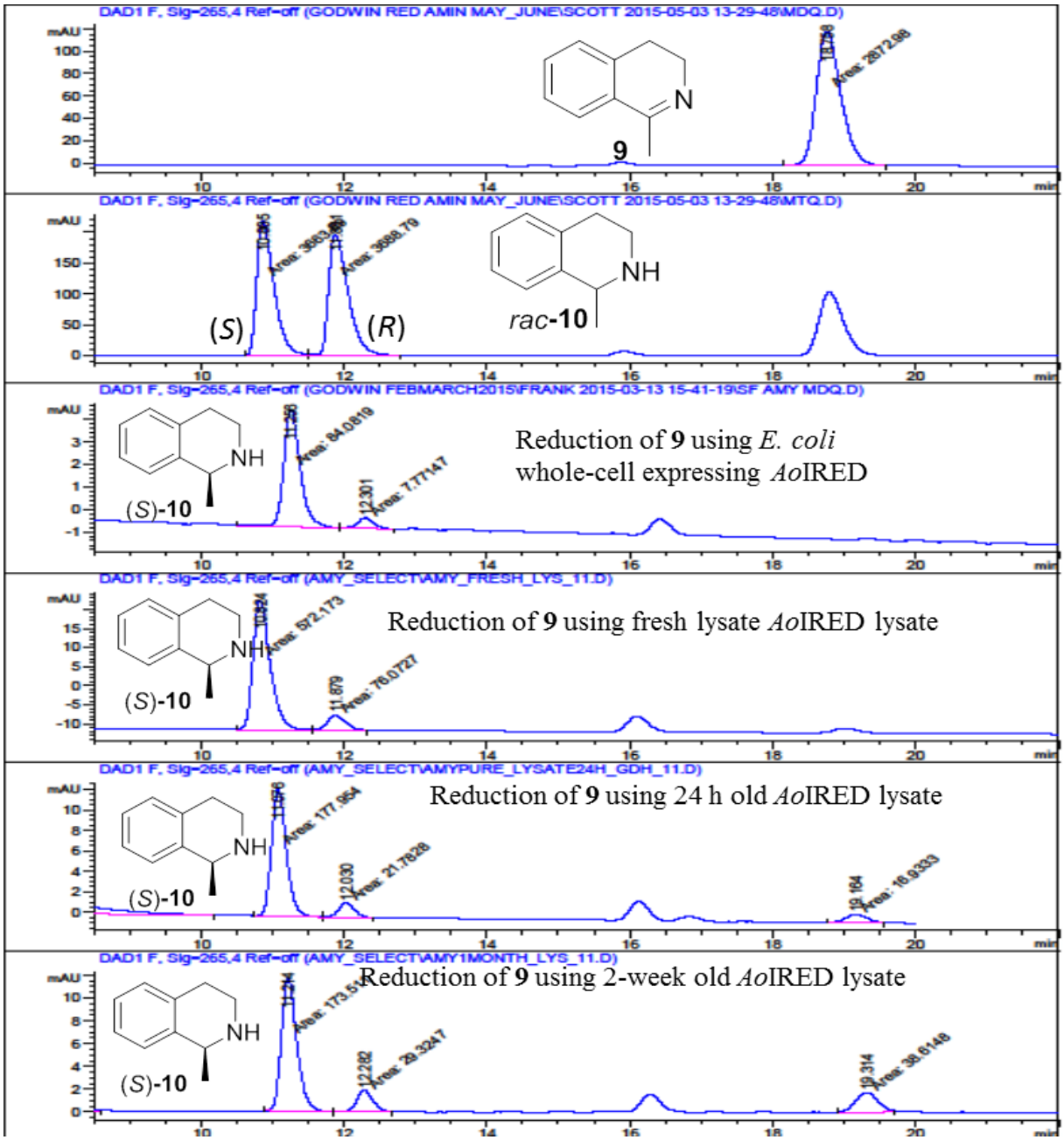

Figure S17. HPLC analysis of *Ao*IRED catalyzed biotransformation of **9**. (Daicel CHIRALPAK®IC 250 mm × 4.6 mm, 5 µm, solvent: hexane/isopropanol/diethylamine = 97/03/0.1, 1 mL/min, 265 nm).

From the top, row 1= standard solution of imine **9**, row 2= standard solution of racemic amine **10**, row 3 =product of biotransformation of **9** using *Ao*IRED whole cell biocatalyst; row 4= product of biotransformation of **9** using fresh *Ao*IRED crude extract (lysate); row 5= product of biotransformation of **9** using 24 h *Ao*IRED crude extract (lysate); row 6 = product of biotransformation of 9 using 2 week old *Ao*IRED crude extract (lysate). *Ao*IRED crude extract (lysate) was stored at 4°C and biotransformation mixtures were incubated at 30°C. Note: the selectivity of *Ao*IRED on **9** was not affected by storage of *Ao*IRED crude extract.

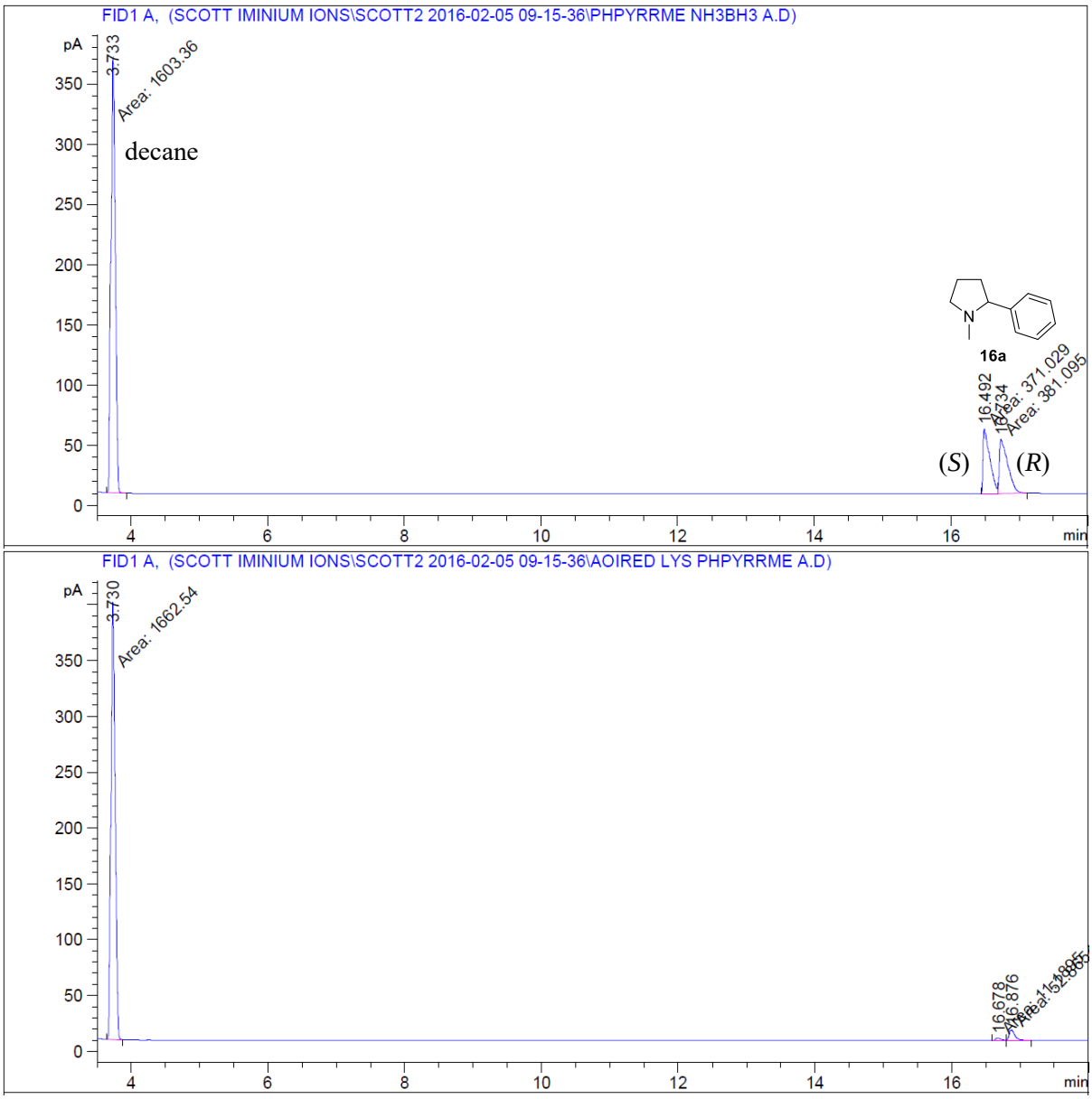
FID1 A, (SCOTT IMINIUM IONS\SCOTT2 2016-02-05 09-15-36\PHPYRRME NH3BH3 A.D)
pA
3.733
Area: 1603.36
decane
16a
16.492
Area: 371.029
16.734
Area: 381.095
(S)
(R)
min
FID1 A, (SCOTT IMINIUM IONS\SCOTT2 2016-02-05 09-15-36\AOIRED LYS PHPYRRME A.D)
pA
3.730
Area: 1662.54
16.678
16.876
min

Figure S18a.

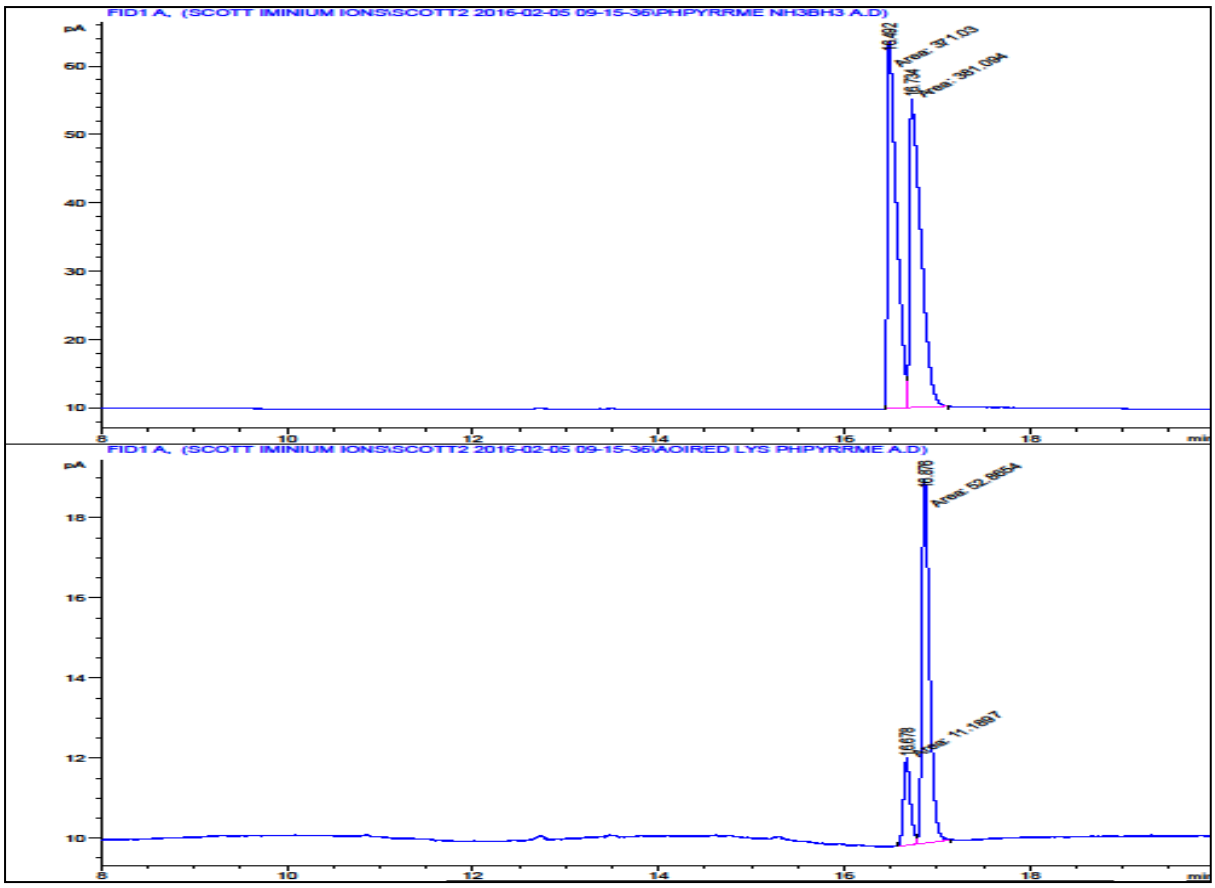

Figure S18b.

Figure S18. **S18a**: GC analysis of *Ao*IRED catalysed biotransformation of **15a**. From the top, row 1= control reaction of **15a** with $NH_3.BH_3$, row 2= fresh *Ao*IRED crude extract (lysate) biotransformation of **15a**. **S18b:** Expansion of separation of enantiomers of **16a** resulting from biotransformation by *Ao*IRED.

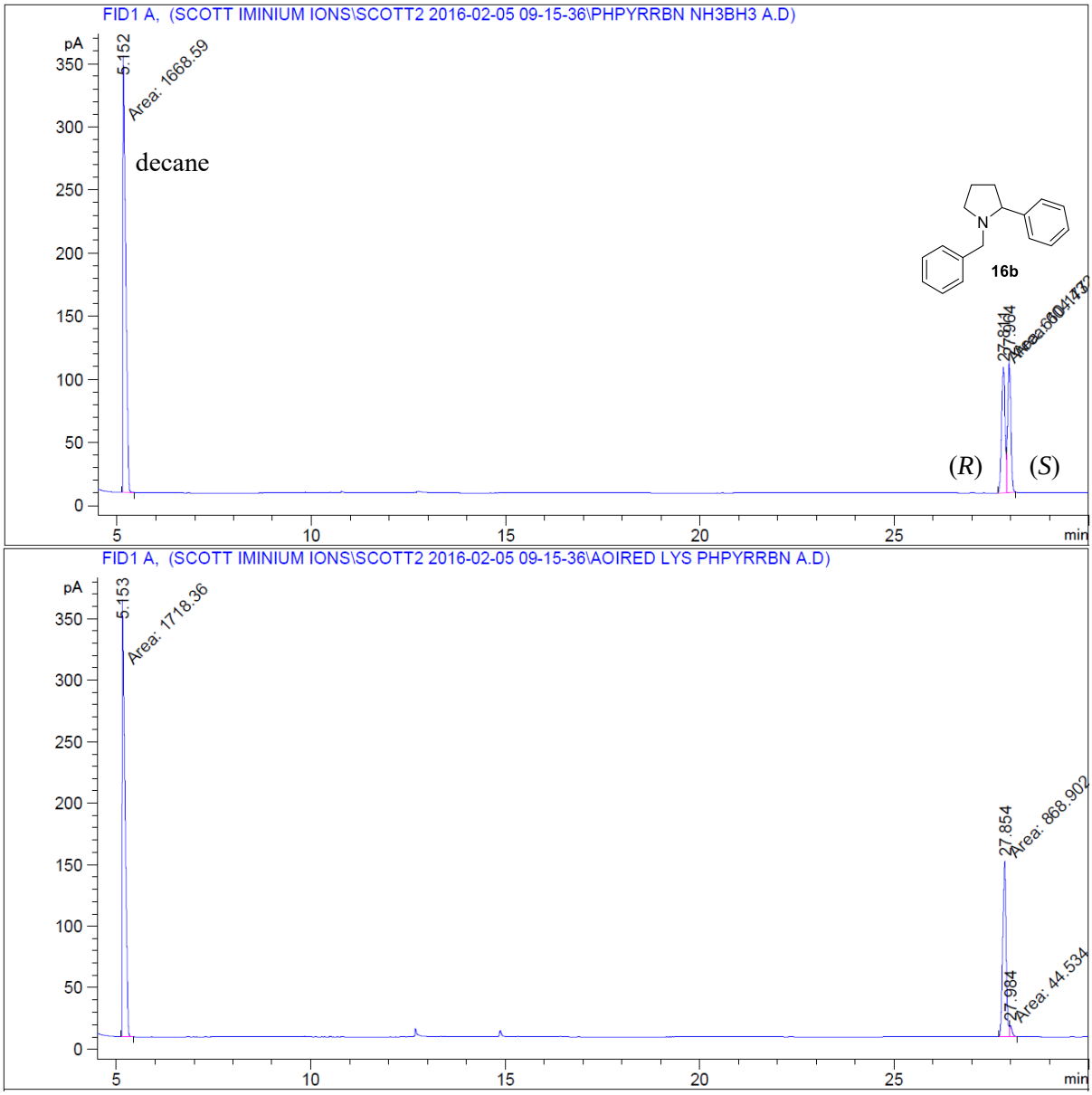

Figure S19. GC analysis of *Ao*IRED catalysed biotransformation of **15b**.

From the top, row 1= control reaction of **15b** with $NH_3.BH_3$, row 2= fresh *Ao*IRED crude extract (lysate) biotransformation of **15b**.

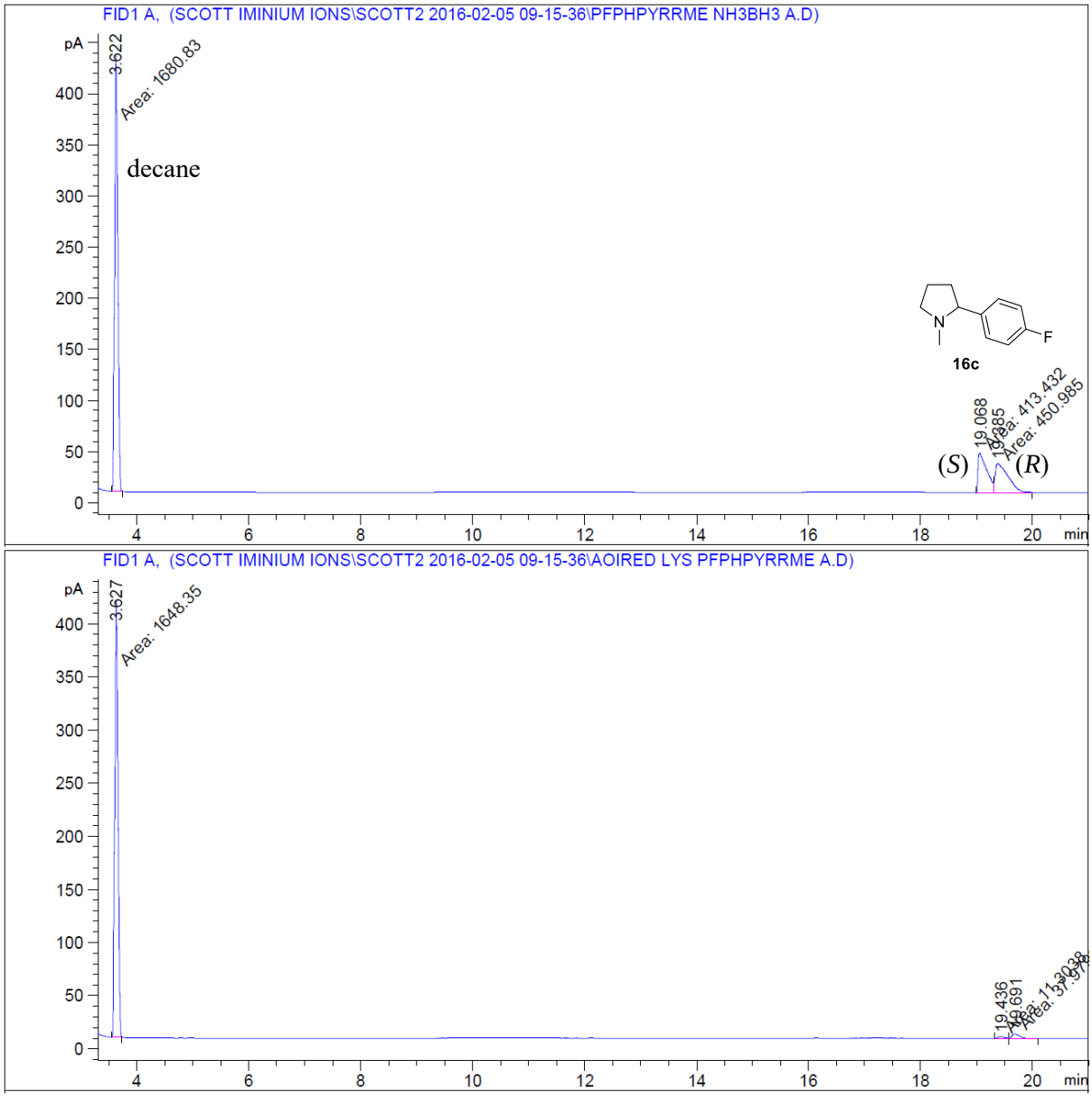

Figure S20.GC analysis of *Ao*IRED catalysed biotransformation of **15c**.

From the top, row 1= control reaction of **15c** with $NH_3.BH_3$, row 2= fresh *Ao*IRED crude extract (lysate) biotransformation of **15c**.

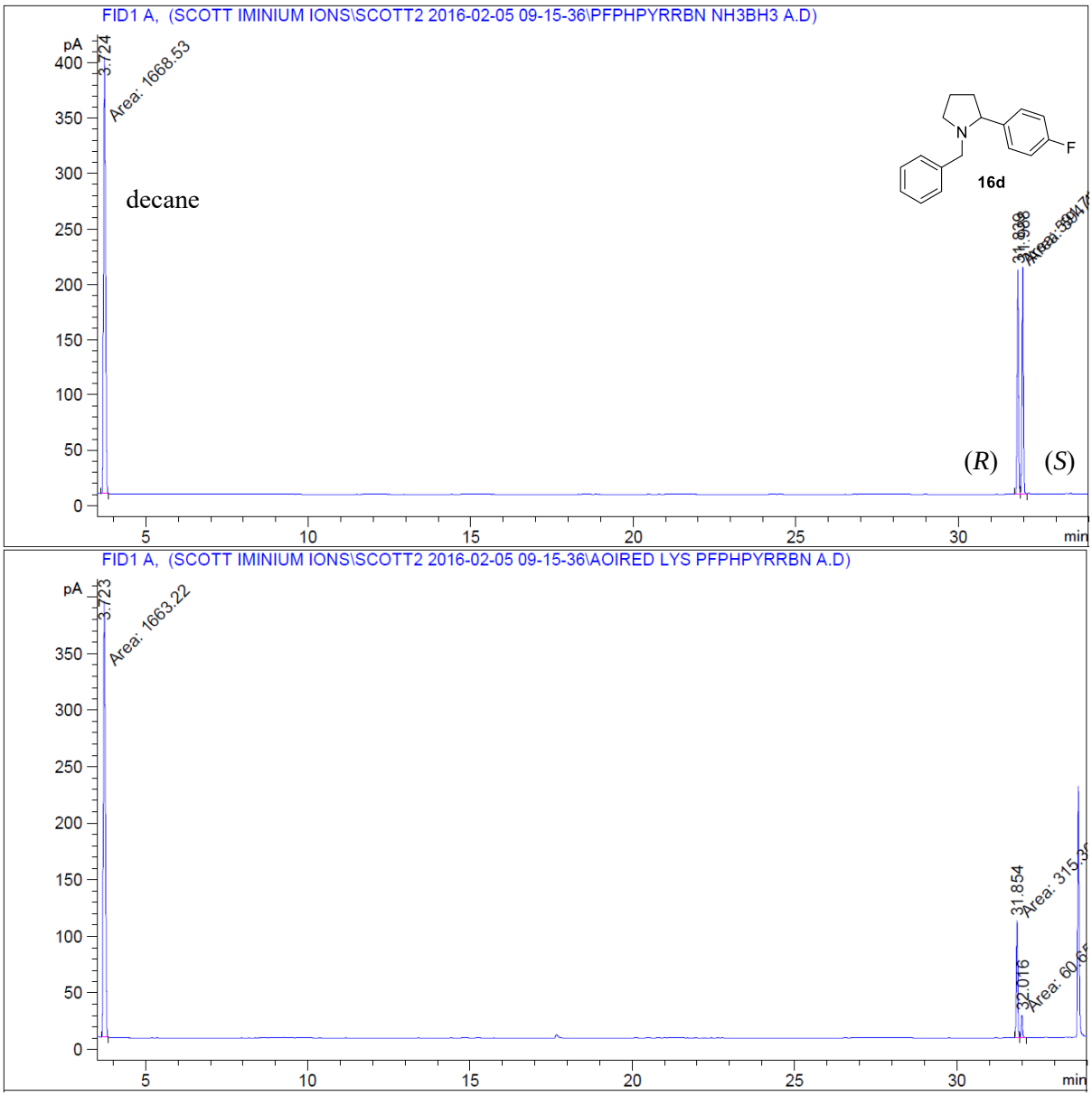
FID1 A, (SCOTT IMINIUM IONS\SCOTT2 2016-02-05 09-15-36\PFPHPYRRBN NH3BH3 A.D)
pA
3.724
Area: 1668.53
decane
16d
F
N
(R)
(S)
min
FID1 A, (SCOTT IMINIUM IONS\SCOTT2 2016-02-05 09-15-36\AOIRED LYS PFPHPYRRBN A.D)
pA
3.723
Area: 1663.22
31.854
32.016
min

Figure S21a.

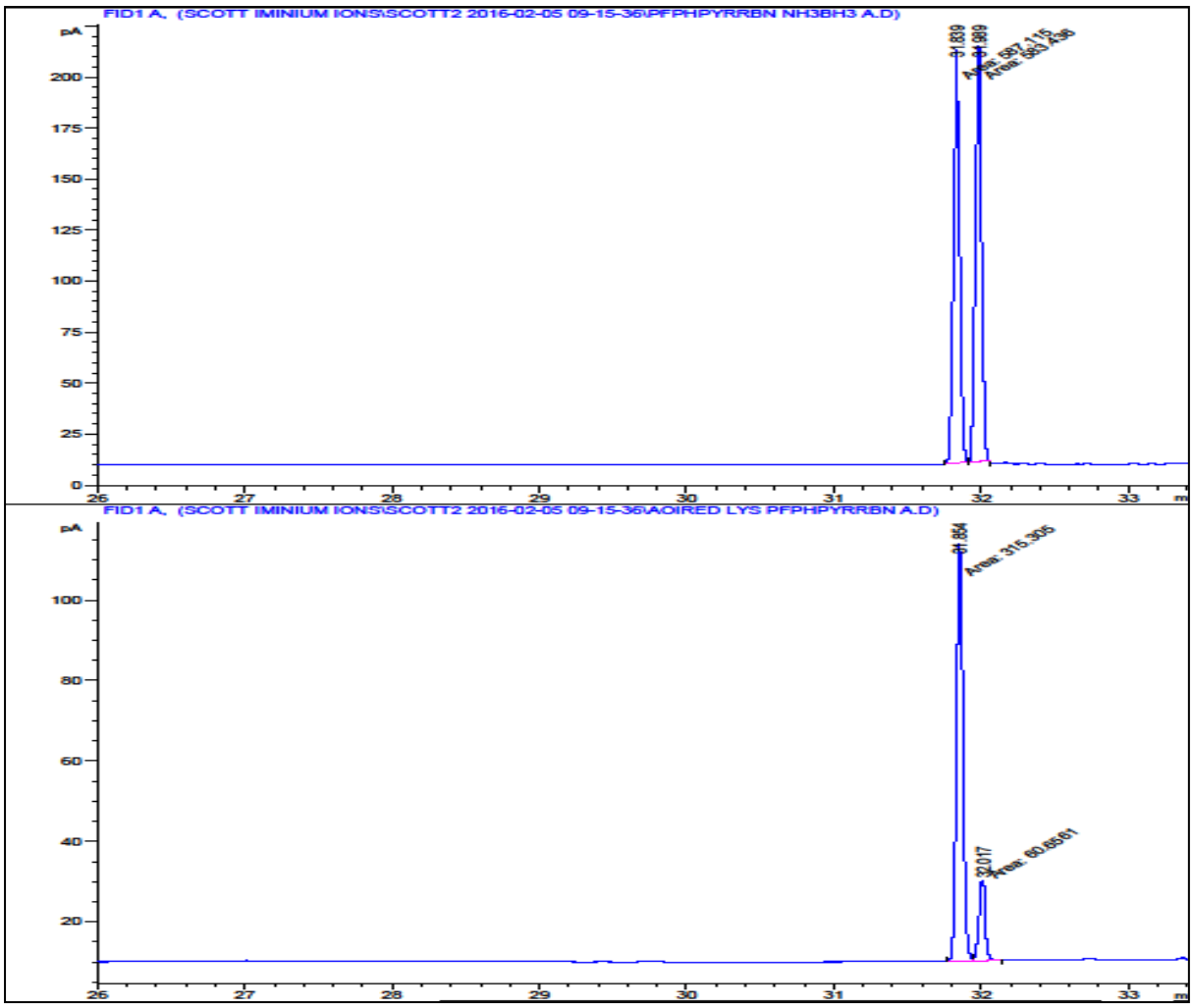

Figure S21b.

Figure S21. **S21a:** GC analysis of *Ao*IRED catalysed biotransformation of **15d**. From the top, row 1= control reaction of **15d** with $NH_3.BH_3$, row 2= fresh *Ao*IRED crude extract (lysate) biotransformation of **15d**. **S21b**. Expansion of separation of enantiomers of **16d** resulting from biotransformation by *Ao*IRED.

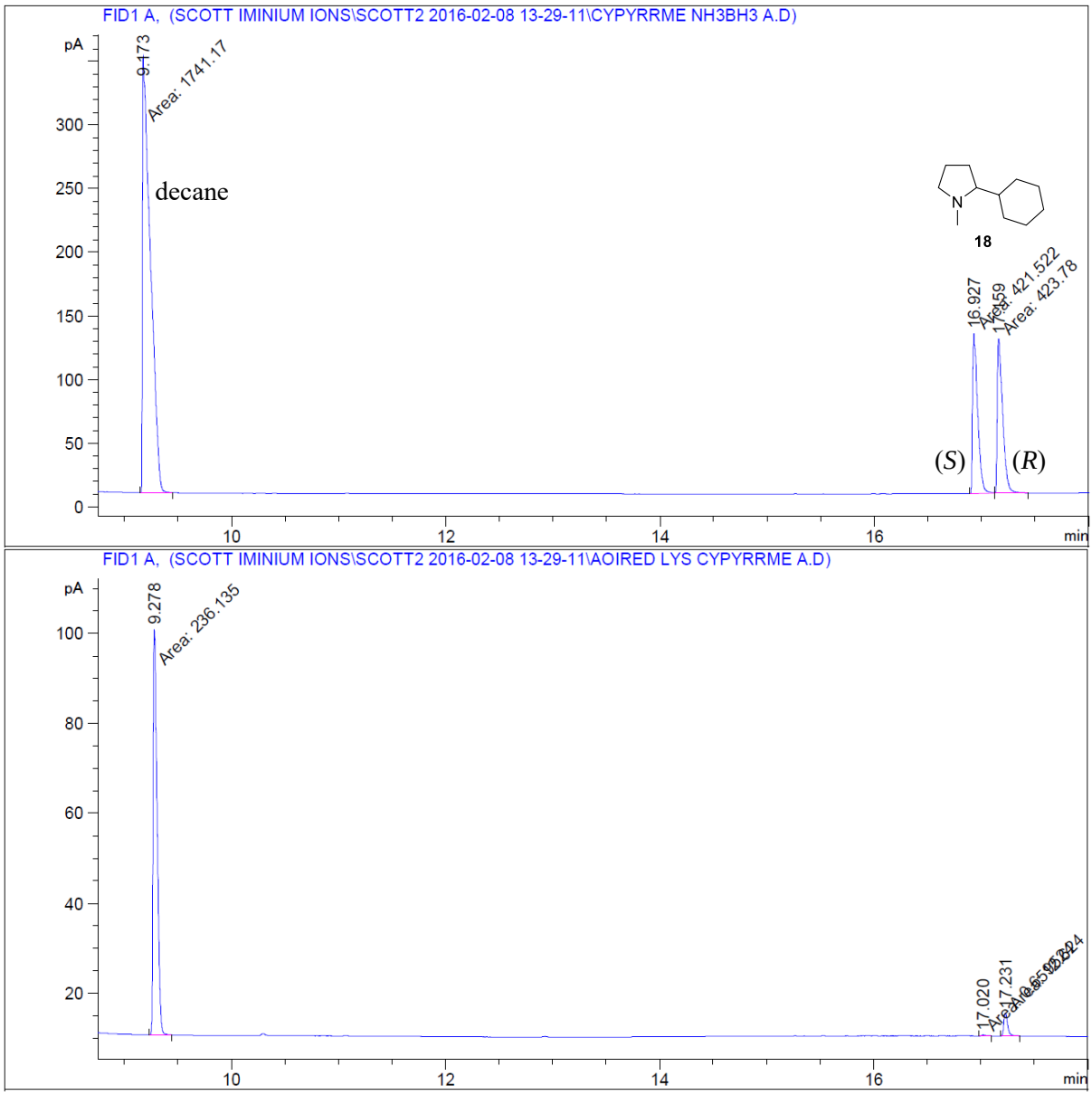

Figure S22. GC analysis of *Ao*IRED catalysed biotransformation of **17**.

From the top, row 1= control reaction of **17** with $NH_3.BH_3$, row 2= fresh *Ao*IRED crude extract (lysate) biotransformation of **17**.

Section S6. X-ray data collection and refinement statistics

Table S4. Data Collection and Refinement Statistics for *Ao*IRED apo-form and in complex with NADPH and (*R*)-MTQ. Numbers in brackets refer to data for highest resolution shells.

	*Ao*IRED *apo*- 'open'	*Ao*IRED NADPH 'closed'	*Ao*IRED (*R*)-MTQ 'closed'
Beamline	Diamond i03	Diamond i04	Diamond i02
Wavelength (Å)	0.97950	0.97935	0.97949
Resolution (Å)	57.78-1.55 (1.59-1.55)	49.29-2.06 (2.11-2.06)	73.78-2.14 (2.20-2.14)
Space Group	$C222_1$	$P2_12_12_1$	$P2_12_12_1$
Unit cell (Å)	a = 75.58; b = 89.62; c = 91.48; α = β = γ = 90°	a = 52.79; b = 66.06; c = 147.88; α = β = γ = 90°	a = 52.85; b = 65.67; c = 147.56; α = β = γ = 90°
No. of molecules in the asymmetric unit	1	2	2
Unique reflections	44372 (3183)	32831 (2401)	29186 (2364)
Completeness (%)	98.1 (96.6)	99.9 (99.9)	99.8 (100.0)
R_{merge} (%)	0.04 (0.70)	0.08 (0.70)	0.05 (0.71)
$R_{p.i.m.}$	0.03 (0.43)	0.05 (0.45)	0.02 (0.28)
Multiplicity	6.7 (6.8)	6.5 (6.4)	6.4 (7.8)
$\langle I/\sigma(I)\rangle$	20.4 (3.1)	17.4 (2.9)	28.3 (4.0)
$CC_{1/2}$	1.00 (0.88)	0.99 (0.80)	0.99 (0.89)
Overall *B* factor from Wilson plot (Å^2)	20	31	21
R_{cryst}/ R_{free} (%)	18.1/21.4	17.3/22.5	17.1/22.4
r.m.s.d 1-2 bonds (Å)	0.022	0.015	0.016
r.m.s.d 1-3 angles (°)	2.12	1.87	1.83
Avge main chain B (Å^2)	23	33	27
Avge side chain B (Å^2)	28	40	31
Avge water B (Å^2)	32	40	33
Avge ligand B (Å^2)	n/a	53	55

Section S7. Structural studies of *Aol*RED

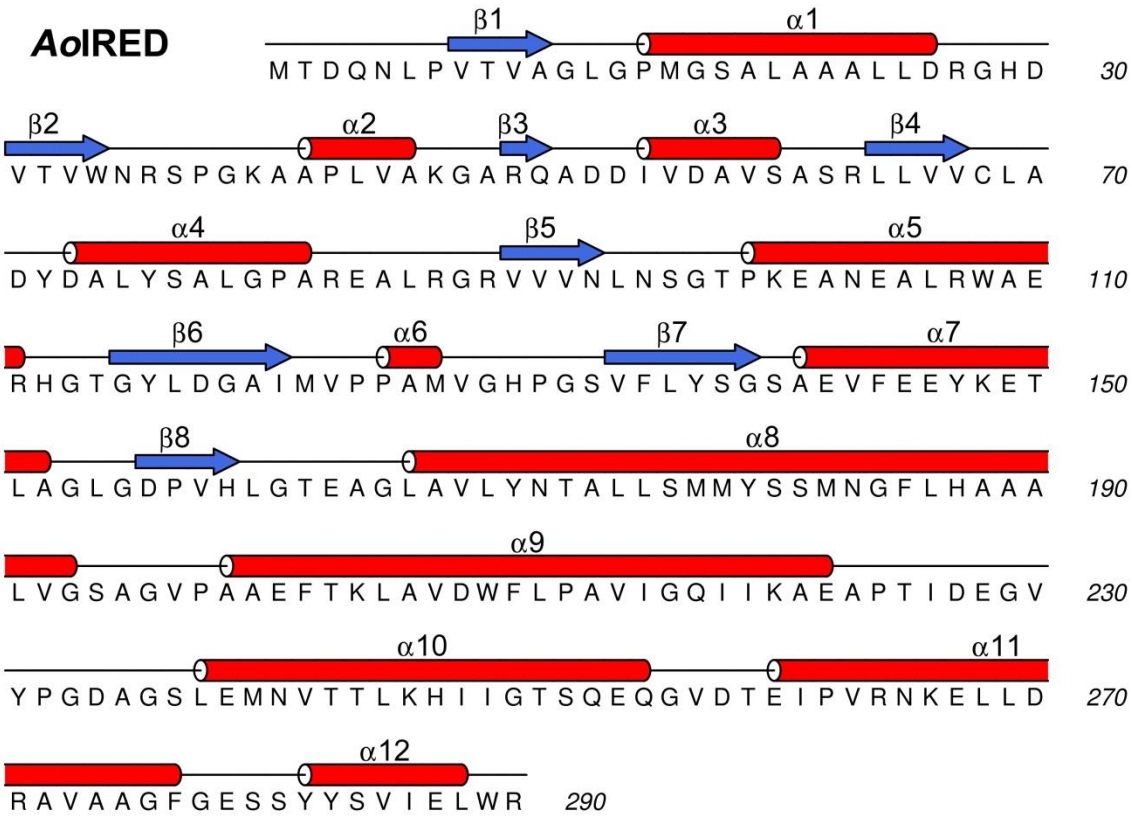

Figure S23. Secondary structural elements of *Ao*IRED, with secondary structure assignment, created using DSSP (*4*,*5*) and represented using ALINE (*6*).

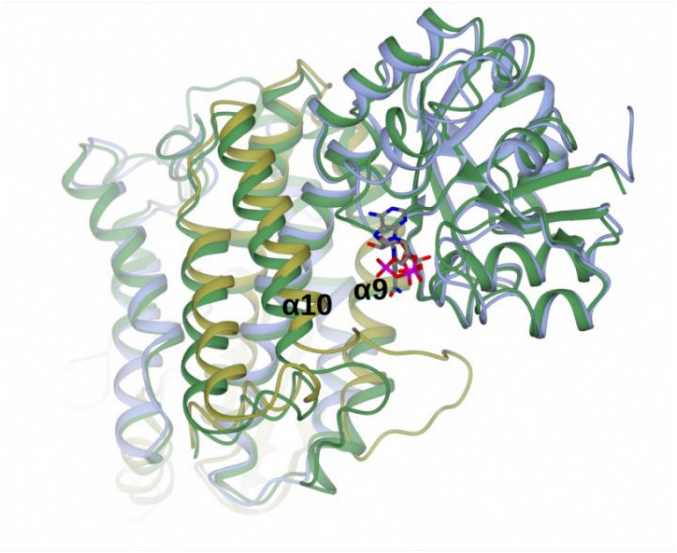

Figure S24. Superimposition of NADPH complex of *Ao*IRED (gold) with the apo form (green), illustrating the loop between α9 and α10 in the C-terminal bundle flipping from the periphery of the enzyme to cover the NADPH binding pocket upon NADP binding**.**

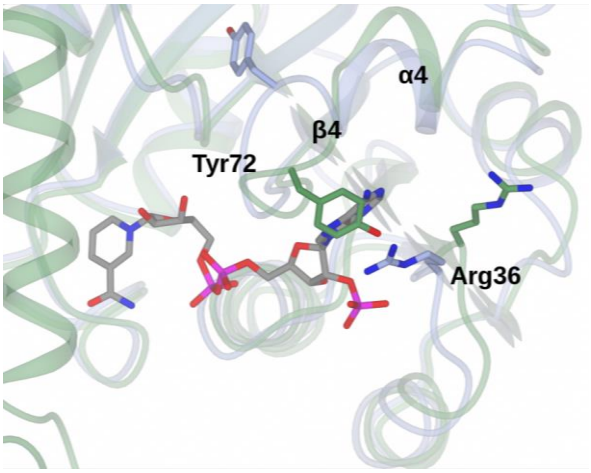

Figure 25. Detail of Superimposition of NADPH complex of *Ao*IRED (light blue) with the *apo*-form (green), and illustrating the movement of loop between α4 and β4 upon NADPH binding. In the NADPH complex, the side chain of Tyr72 has moved away from the ADP binding pocket to the interior of the Rossman domain; Arg36 has moved in to interact with the ADP ribose 2' phosphate.

Section S8. Analysis of *Ao*IRED mutants

Table S5. Biotransformation of imine substrates using WT *Ao*IRED and variants at Y179

Imine	Amine	*Ao*IRED WT			*Ao*IRED Y179A			*Ao*IRED Y179F		
		Conv. (%)	e.e (%)	(*R*/*S*)	Conv. (%)	e.e (%)	(*R*/*S*)	Conv. (%)	e.e (%)	(*R*/*S*)
1a	**2a**	96	82	(*S*)-	23	>99	(*S*)-	35	47	(*S*)-
1b	**2b**	100	95	(*S*)-	8	>99	(*S*)-	99	92	(*S*)-
1c	**2c**	98	>99	(*S*)-	0	n/a	*n/a*	90	>99	(*S*)-
1d	**2d**	85	>99	(*R*)-	2	>99	(*R*)-	0	n/a	*n/a*
3b	**4b**	>99	40	(*S*)-	32	43	(*R*)-	93	8	(*R*)-
3c	**4c**	>99	60	(*R*)-	10	54	(*R*)-	90	44	(*R*)-
3d	**4d**	77	90	(*R*)-	3	59	(*R*)-	25	84	(*R*)-
5a	**6a**	95	99	(*S*)-	69	>99	(*S*)-	10	60	(*R*)-
7	**8**	100	n/a	*n/a*	100	n/a	*n/a*	81	n/a	*n/a*
9	**10**	100	98	(*S*)-	100	>98	(*R*)-	99	65	(*R*)-
11	**12**	50	79	(*S*)-	15	>99	(*R*)-	5	>99	(*R*)-
13c	**13c**	15	62	(*S*)-	10	>99	(*S*)-	9	>99	(*S*)-
19a	**20a**	100	n/a	*n/a*	33	n/a	*n/a*	80	n/a	*n/a*
19b	**20b**	17	48	(*R*)-	2	10	(*S*)-	56	>99	(*R*)-

n/a = not applicable

Table S6. Biotransformation of imine substrates catalyzed by WT *Ao*IRED and N241A mutant.

		*Ao*IRED WT			*Ao*IRED N241A		
Imine	Amine	Conv. (%)	e.e. (%)	(*R*/*S*)	Conv. (%)	ee (%)	(*R*/*S*)
1a	**2a**	96	82	(*S*)-	43	81	(*S*)-
1b	**2b**	100	95	(*S*)-	96	>99	(*S*)-
3b	**4b**	>99	40	(*S*)-	>99	0	*rac*-
3c	**4c**	>99	60	(*R*)-	99	46	(*R*)-
3d	**4d**	77	90	(*R*)-	56	72	(*R*)-
7	**8**	100	n/a	n/a	100	n/a	n/a
9	**10**	100	98	(*S*)-[a]	100	71	(*R*)-
11	**12**	50	79	(*S*)-	>99	85	(*R*)-
13c	**14c**	15	62	(*S*)-	96	60	(*R*)-

[a] Inversion of selectivity was observed using a 24 h old aliquot of *Ao*IRED**,** results from biotransformations using freshly purified *Ao*IRED are presented. n/a= not applicable.

Table S7. Biotransformations of imine substrates using WT *Ao*IRED and variants at N171**.**

		*Ao*IRED WT			*Ao*IRED N171A			*Ao*IRED N171D		
Imine	Amine	Conv. (%)	e.e. (%)	(*R*/*S*)	Conv. (%)	e.e. (%)	(*R*/*S*)	Conv. (%)	e.e. (%)	(*R*/*S*)
1a	**2a**	96	82	(*S*)-	31	>99	(*S*)-	2.3	>99	(*S*)-
1b	**2b**	100	95	(*S*)-	99.6	4	(*S*)-	100	95	(*S*)-
1c	**2c**	98	>99	(*S*)-	12	98	(*S*)-	11	>99	(*S*)-
1d	**2d**	85	>99	(*R*)-	57	>99	(*R*)-	98	>99	(*R*)-
3a	**4a**	>99	98	(*S*)-	64	15	(*S*)-	58	83	(*S*)-
3b	**4b**	>99	40	(*S*)-	41	68	(*S*)-	80	80	(*S*)-
3c	**4c**	100	60	(*R*)-	46	26	(*S*)-	23	34	(*S*)-
3d	**4d**	77	90	(*R*)-	2	>99	(*R*)-	11	80	(*R*)-
3e	**4e**	>99	>99	(*R*)-	86	61	(*R*)-	69	52	(*R*)-
7	**8**	100	n/a	*n/a*	21	n/a	*n/a*	15	n/a	*n/a*
9	**10**	100	98	(*R*)-	36	11	(*S*)-	30	66	(*R*)-
11	**12**	50	79	(*S*)-	2	31	(*S*)-	2.0	>99	(*S*)-
13c	**14c**	15	62	(*S*)-	18	71	(*S*)-	6	>99	(*S*)-
19a	**20a**	100	n/a	*n/a*	84	n/a	*n/a*	58	n/a	*n/a*
19b	**20b**	17	48	(*R*)-	41	95	(*S*)-	2.3	13	(*R*)-

n/a= not applicable

Table S8. Kinetic parameters of WT *Ao*IRED and variants at Y179.

	*Ao*IRED WT			*Ao*IRED Y179A			*Ao*IRED Y179F		
Imine	K_m (mM)	k_{cat} (s^{-1})	k_{cat}/K_m (s^{-1} mM^{-1})	K_m (mM)	k_{cat} (s^{-1})	k_{cat}/K_m (s^{-1} mM^{-1})	K_m (mM)	k_{cat} (s^{-1})	k_{cat}/K_m (s^{-1} mM^{-1})
1a	0.87 ± 0.43	0.15 ± 0.08	0.17 ± 0.18	1.77 ± 0.88	0.03 ±0.01	0.05 ±0.01	0.87 ± 0.25	0.01 ± 0.00	0.02 ± 0.01
7	0.36 ± 0.04	0.94 ± 0.01	2.58 ± 0.30	0.39 ± 0.10	1.52 ± 0.09	3.95 ±0.90	0.85 ± 0.02	0.32 ± 0.03	0.38 ± 0.20
9	0.72 ± 0.05	0.74 ± 0.02	1.03 ± 0.40	0.45 ± 0.07	0.92 ±0.02	2.03 ±0.29	0.19 ± 0.02	0.07 ± 0.00	0.36 ± 0.05

Table S9. Kinetic parameters of WT *Ao*IRED and N241A.

	*Ao*IRED WT			*Ao*IRED N241A		
Imine	K_m (mM)	k_{cat} (s^{-1})	k_{cat}/K_m (s^{-1} mM^{-1})	K_m (mM)	k_{cat} (s^{-1})	k_{cat}/K_m (s^{-1} mM^{-1})
1a	0.87 ± 0.43	0.15 ± 0.08	0.17 ± 0.18	1.27 ±0.66	0.22 ± 0.08	0.17 ± 0.10
7	0.36 ± 0.04	0.94 ± 0.01	2.58 ± 0.30	0.47 ± 0.12	0.95 ± 0.06	2.02 ± 0.49
9	0.72 ± 0.05	0.74 ± 0.02	1.03 ± 0.40	0.83 ± 0.20	0.76 ± 0.05	0.92 ± 0.25

Table S10. Kinetic parameters of WT *Ao*IRED and variants at N171.

	*Ao*IRED WT			*Ao*IRED N171A			*Ao*IRED N171D		
Imine	K_m (mM)	k_{cat} (s^{-1})	k_{cat}/K_m (s^{-1} mM^{-1})	K_m (mM)	k_{cat} (s^{-1})	k_{cat}/K_m (s^{-1} mM^{-1})	K_m (mM)	k_{cat} (s^{-1})	k_{cat}/K_m (s^{-1} mM^{-1})
1a	0.87 ± 0.43	0.15 ± 0.08	0.17 ± 0.18	7.90 ± 2.35	0.12 ± 0.01	0.02 ± 0.00	2.22 ± 0.39	0.17 ± 0.10	0.01 ± 0.00
7	0.36 ± 0.04	0.94 ± 0.01	2.58 ± 0.30	1.90 ± 0.77	0.15 ± 0.04	0.08 ± 0.06	1.44 ± 0.65	0.15 ± 0.03	0.10 ± 0.03
9	0.72 ± 0.05	0.74 ± 0.02	1.03 ± 0.40	3.15 ± 0.01	0.01 ± 0.00	0.01 ± 0.19	0.72 ± 0.20	0.21 ± 0.0	0.30 ± 0.02

Section S9. References

(1) Hussain, S.; Leipold, F.; Man, H.; Wells, E.; France, S.; Mulholland, K.R.; Grogan, G.; Turner, N.J. *Chemcatchem*, **2015**, *7,* 579-583.

(2) Leipold, F.; Hussain, S.; Ghislieri, D.; Turner, N.J. *Chemcatchem* **2013**, *5*, 3505-3508.

(3) Hou, G.-H.; Xie, J.-H.; Yan, P.-C.; Zhou, Q.-L. *J. Am. Chem. Soc.* **2009**, *131*, 1366-1367.

(4) Joosten, R.P.; Te Beek, T.A.H.; Krieger, E.; Hekkelman, M.L.; Hooft, R.W.W.; Schneider, R.; Sander, C.; Vriend, G. *Nucl. Acids. Res.* **2011** *39*, 411-419.

(5) Kabsch, W.; Sander, C. *Biopolymers*. **1983,** *22*, 2577-2637.

(6) Bond, C.S.; Schüttelkopf, A.W. *Acta Crystallogr. Sect. D Biol. Crystallogr.* **2009**, *65*, 510-512.